

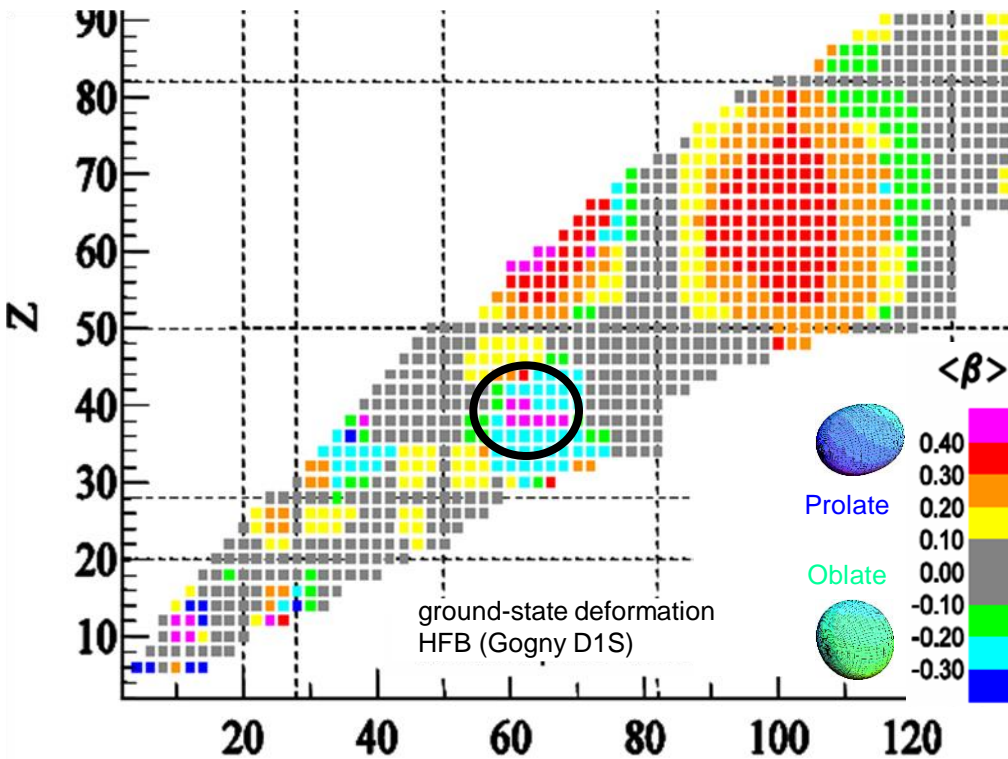
# Nuclear Shapes

## Lecture III

Andreas Görzen  
Department of Physics  
University of Oslo, Norway  
[andreas.gorgen@fys.uio.no](mailto:andreas.gorgen@fys.uio.no)

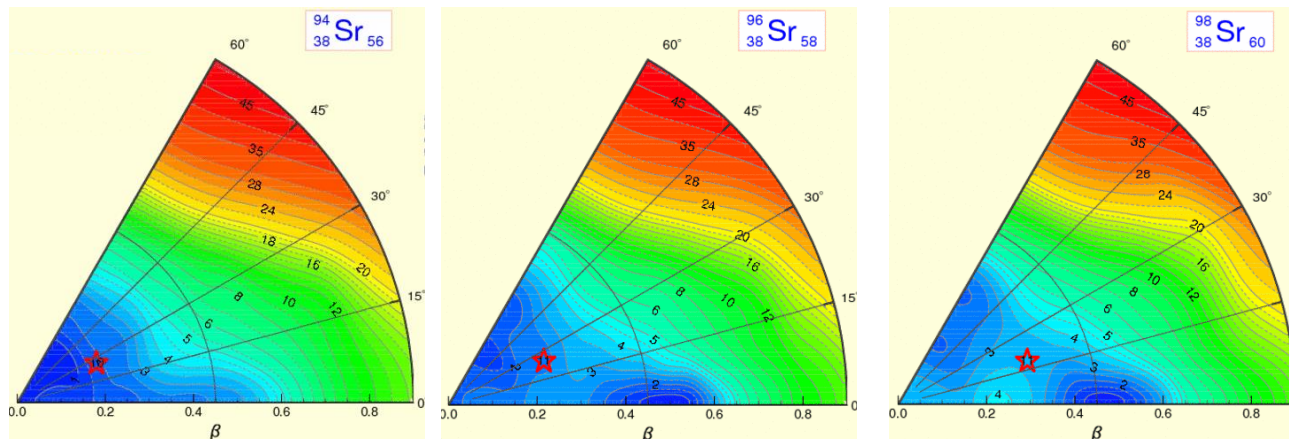
Selected Topics in Nuclear and Atomic Physics  
Fiera di Primiero  
2.-6. October 2017

# Shapes and shape transitions in the nuclear chart

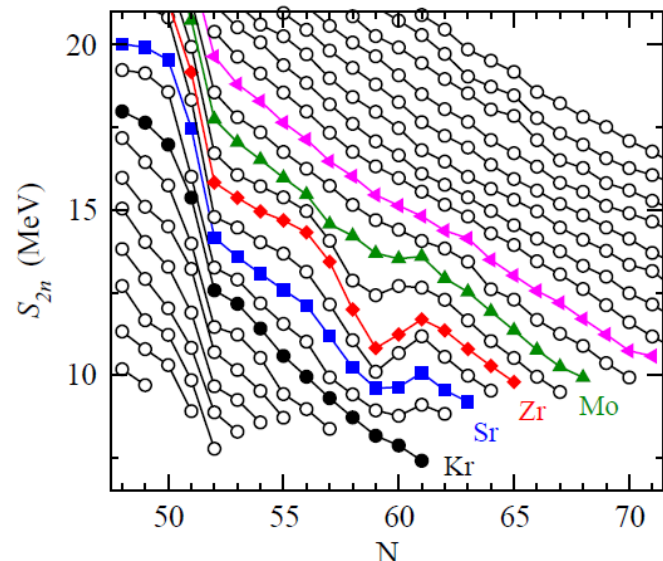
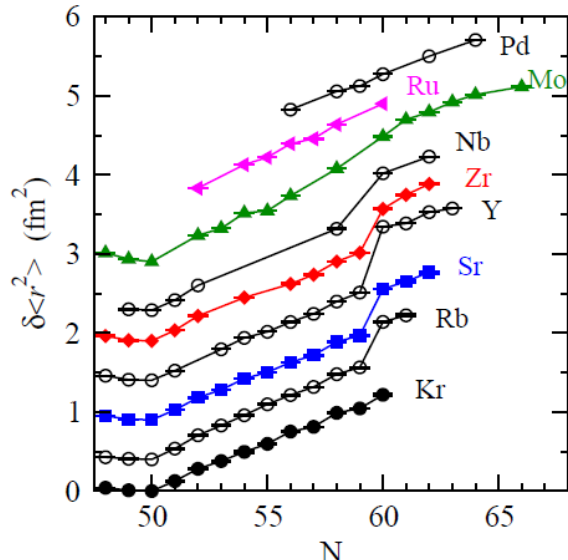
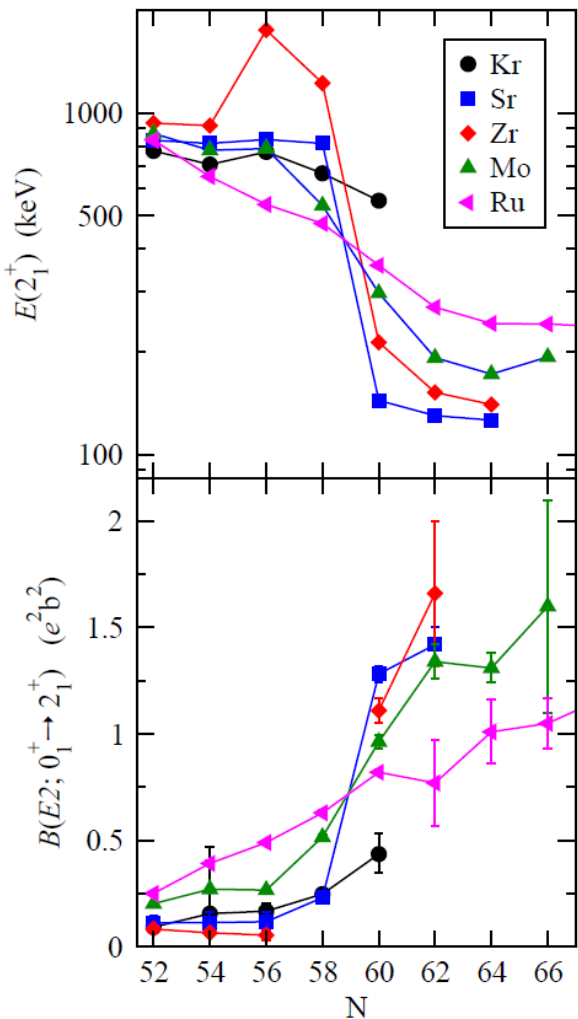


- rapid changes in the ground-state deformation for  $Z \approx 40$  and  $N \approx 60$
- shape coexistence in the regions of shape transition
- observables related to nuclear shape: quadrupole moments,  $B(E2)$  values
- benchmarks for theory

<http://www-phynu.cea.fr/>  
S.Hilaire, M.Girod, Eur. Phys. J. A 33, 237 (2007)



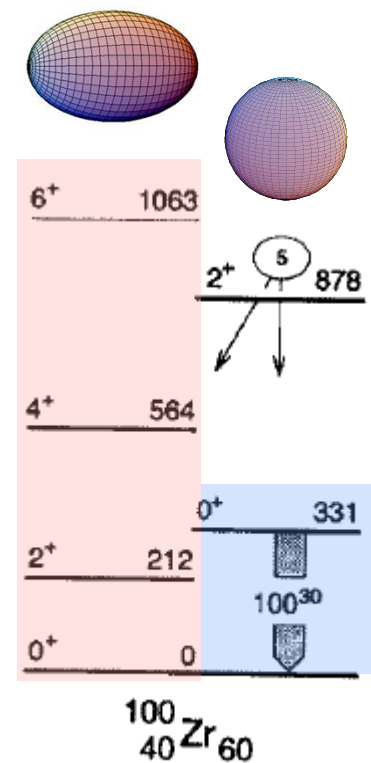
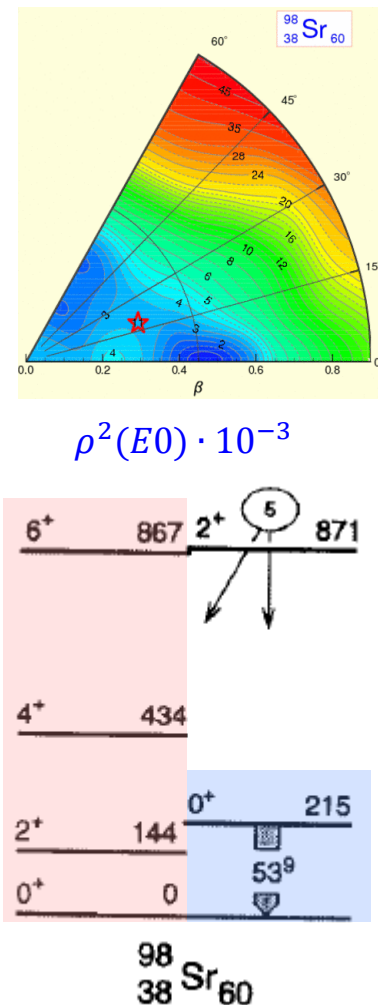
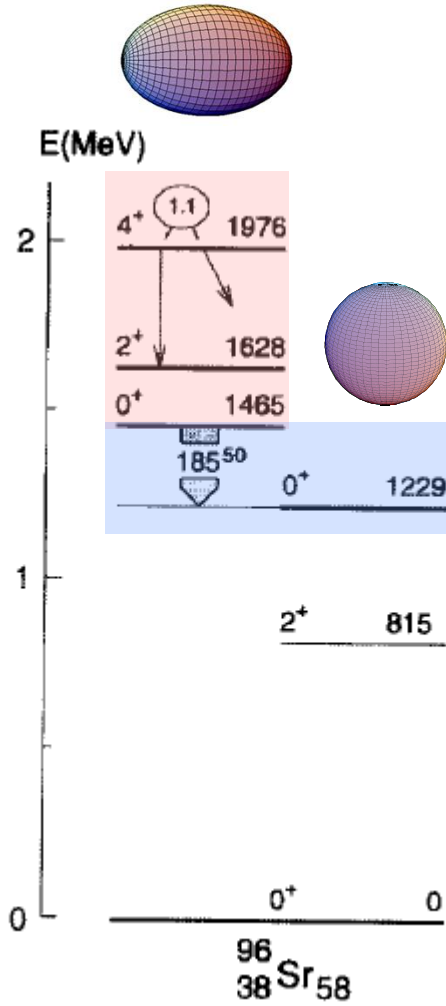
# Shape transition at $N = 60$



At  $N = 60$ :

- drop in energy of first  $2^+$  state
- steep increase of  $B(E2; 0^+ \rightarrow 2^+)$
- discontinuity in charge radii
- irregularity in two-neutron binding energy

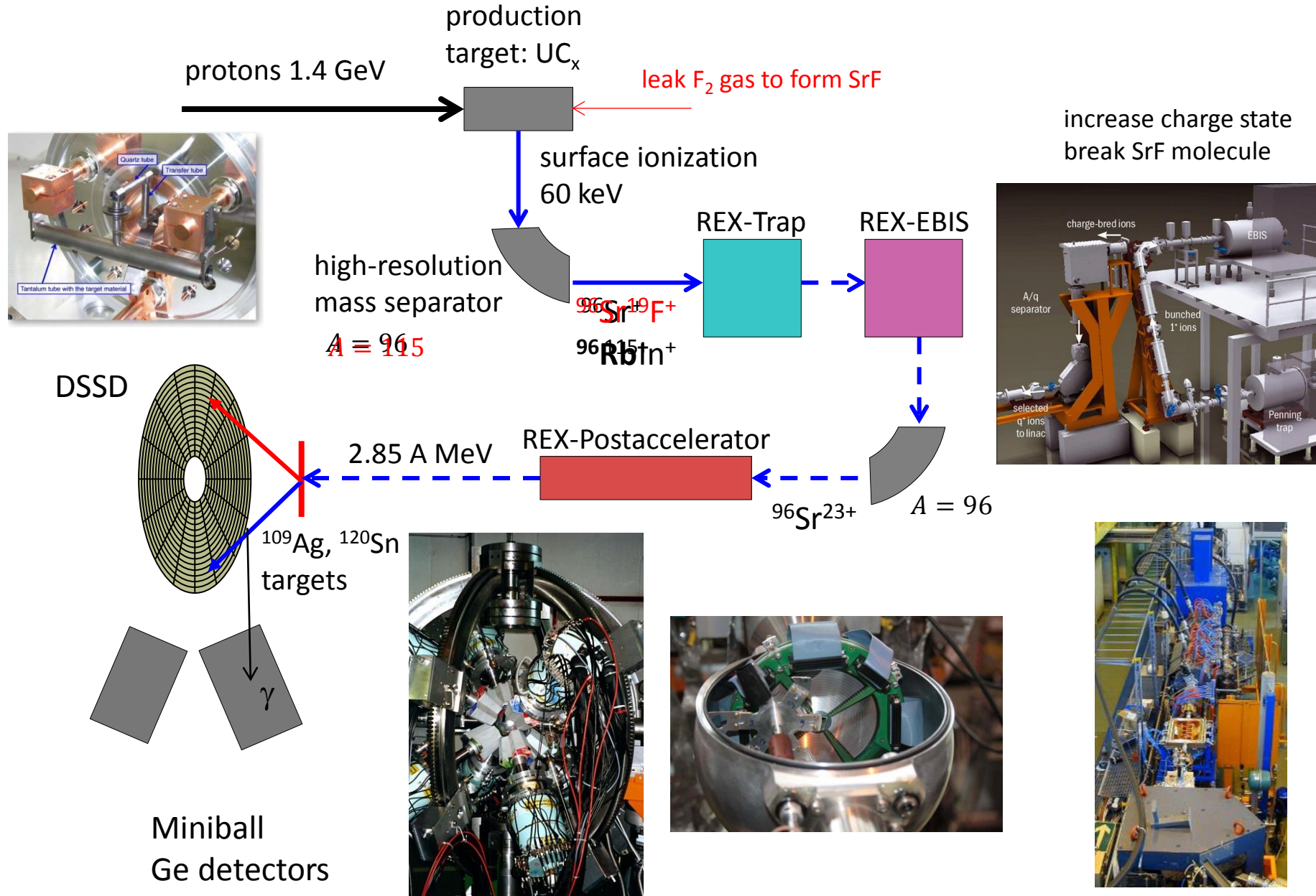
# $E0$ transitions in Sr and Zr isotopes at $N \approx 60$



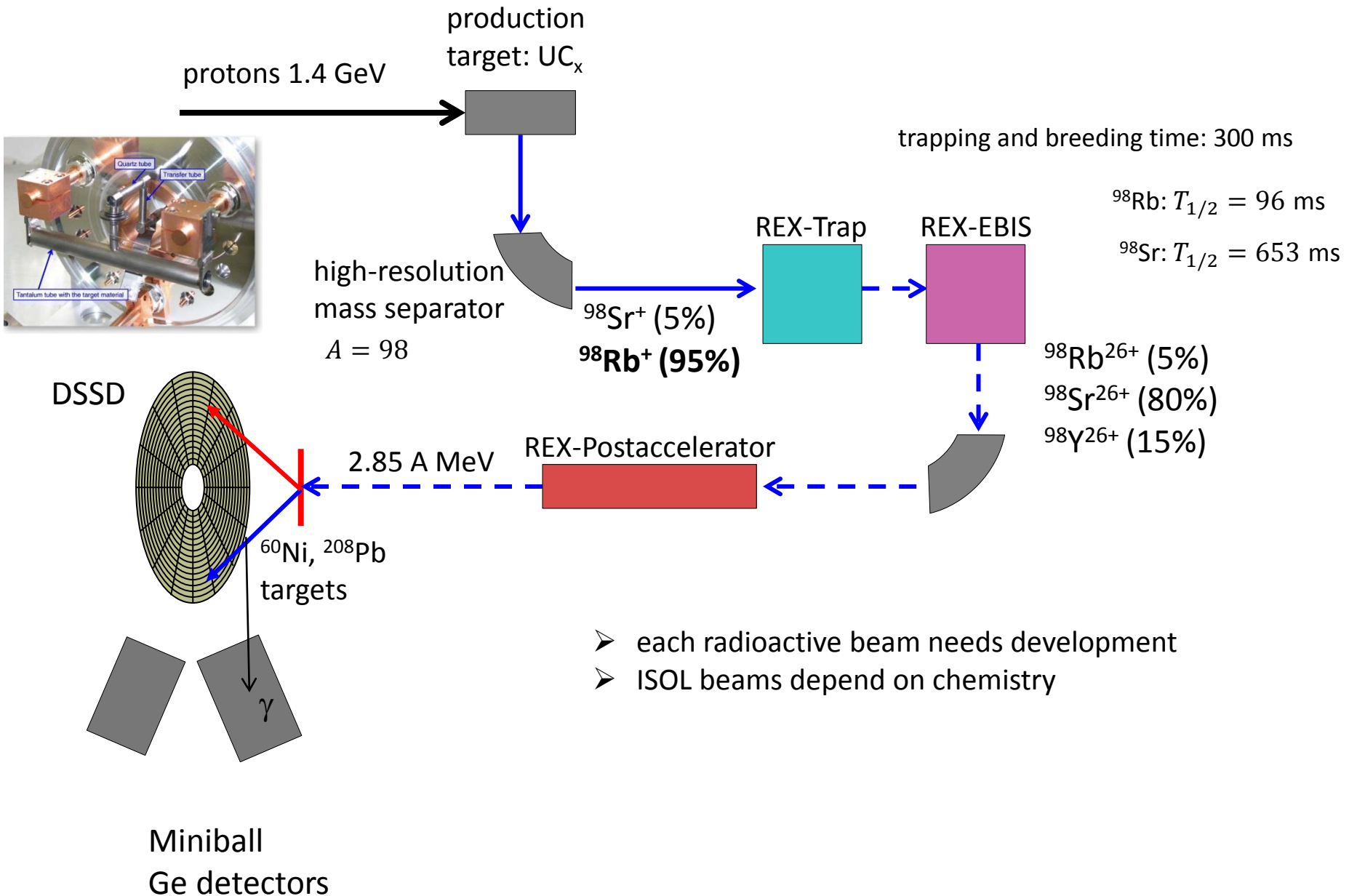
- rotational band
- low-lying  $0_2^+$  state with large  $\rho^2(E0)$

J.L. Wood et al.,  
Nucl. Phys. A 651, 323 (1999)

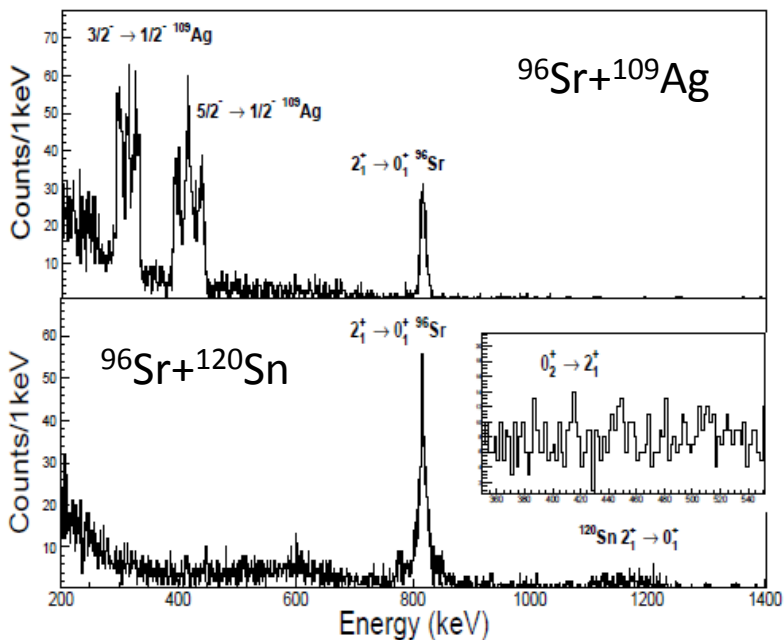
# Isotope separation on-line and postacceleration at CERN-ISOLDE



# Isotope separation on-line and postacceleration at CERN-ISOLDE

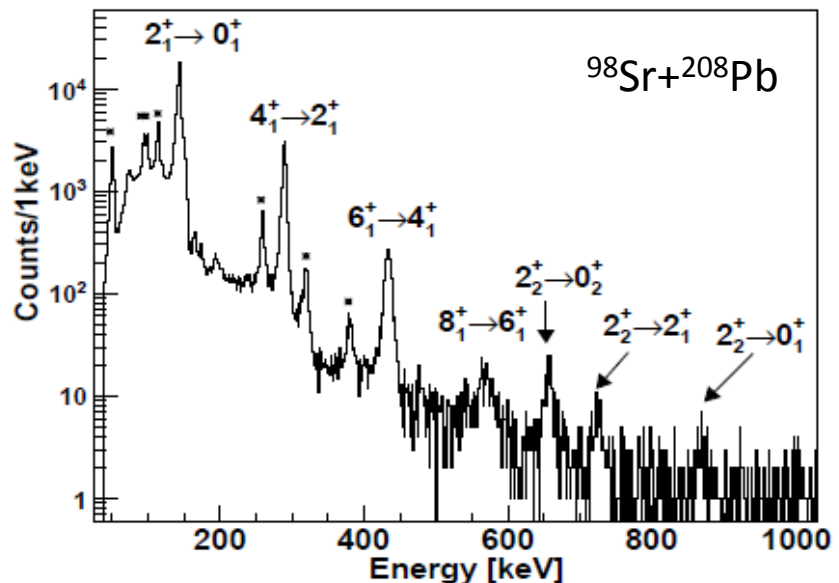
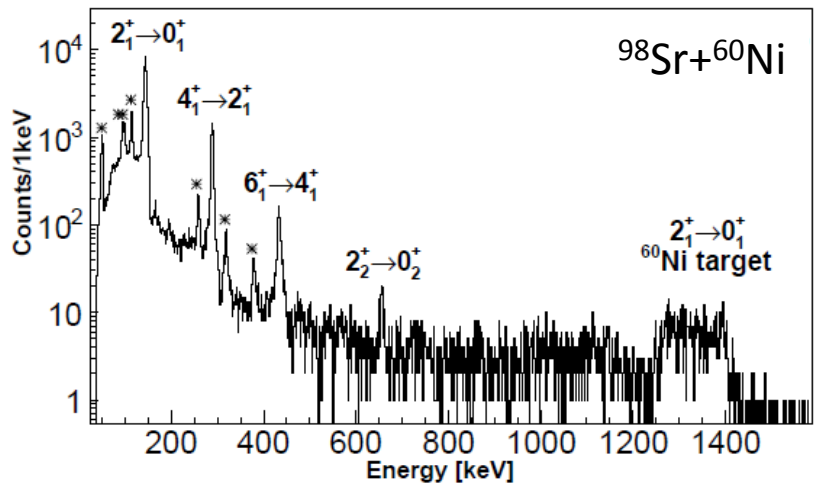


# Coulomb excitation of $^{96,98}\text{Sr}$ at CERN – ISOLDE



Doppler correction for projectiles  
normalization to known  $B(E2)$  values in target

Coulomb excitation probabilities:  
(as function of  $\theta$  and  $Z$ )  
⇒  $B(E2)$  values  
⇒ spectroscopic quadrupole moments  $Q_s$   
(reorientation effect)

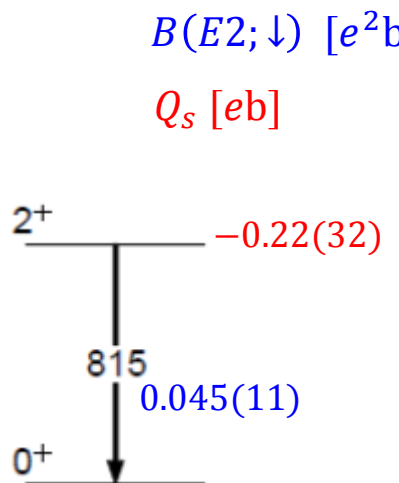


E. Clément et al.  
Phys.Rev.Lett. 116, 022701 (2016)  
Phys.Rev. C 94, 054326 (2016)

# Coulomb excitation of $^{98}\text{Sr}$ at CERN – ISOLDE

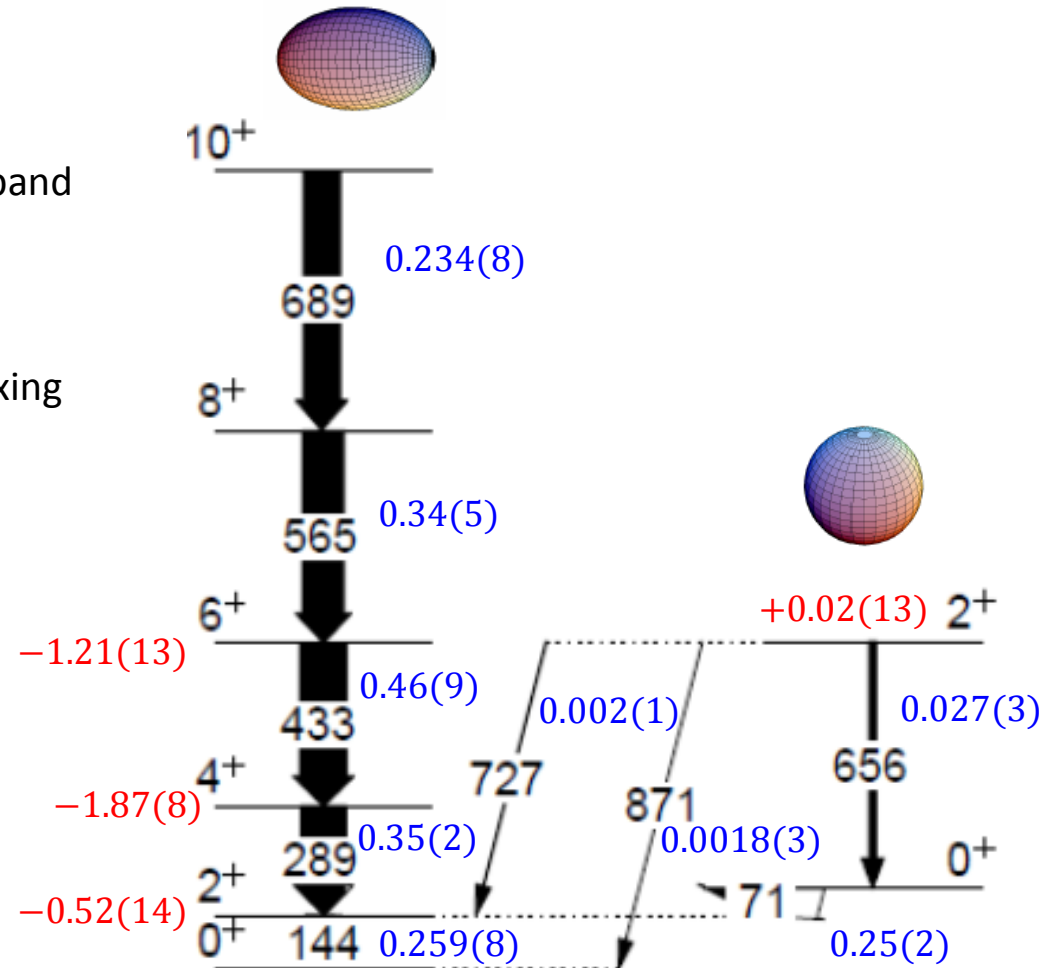
## $^{98}\text{Sr}$

- rotational behavior of ground-state band
- excited configuration similar to  $^{96}\text{Sr}$
- quadrupole moments confirm shape coexistence
- $B(E2; 2_2^+ \rightarrow 0_1^+)$  indicates strong mixing



## $^{96}\text{Sr}$

- $Q_s(2_1^+) \approx 0$   
⇒ no static quadrupole deformation
- sizeable  $B(E2)$   
⇒ vibrational character of  $2_1^+$

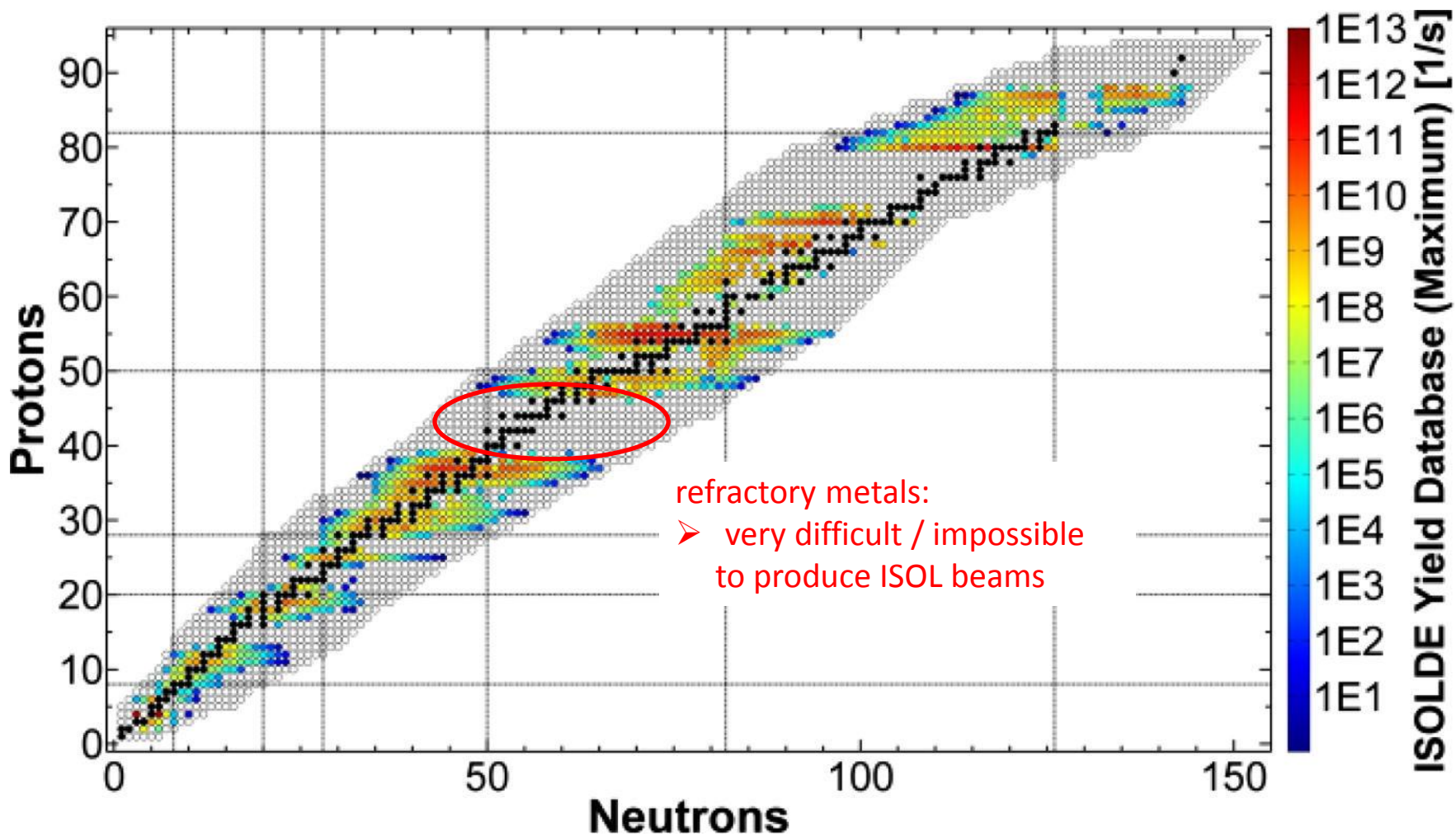


E. Clément et al.

Phys. Rev. Lett. 116, 022701 (2016)

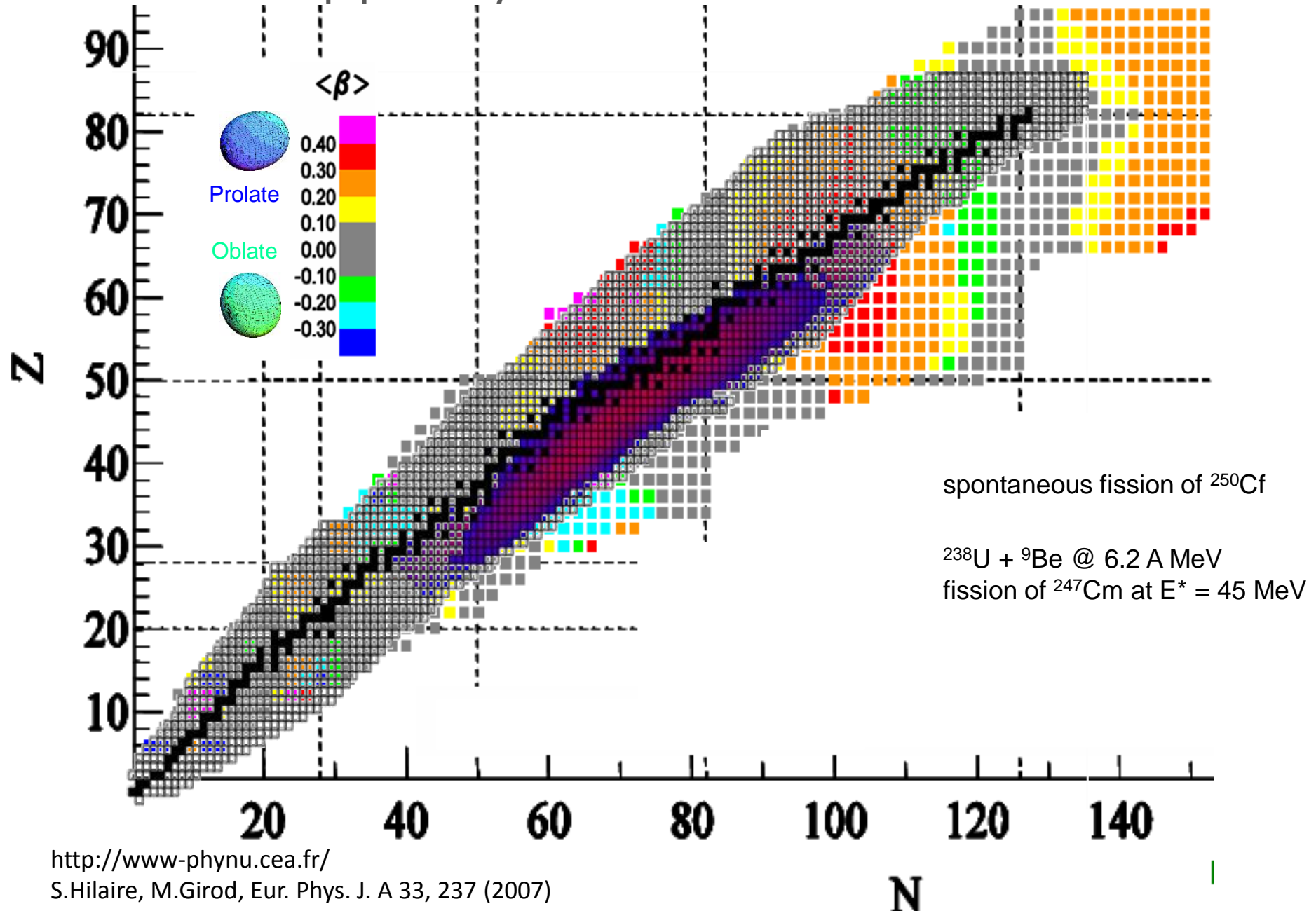
Phys. Rev. C 94, 054326 (2016)

## ISOL beams produced at CERN-ISOLDE



this is a region of dramatic shape transitions  
and shape coexistence !

# Neutron-rich nuclei populated by fission



# Heavy-ion induced fission experiments with VAMOS

April 2011

${}^9\text{Be}({}^{238}\text{U}, \text{f}) {}^{247}\text{Cm}$   
fusion-fission reaction

20°

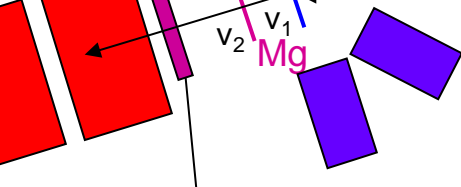
Q

Q

D

8x90°

3x135°

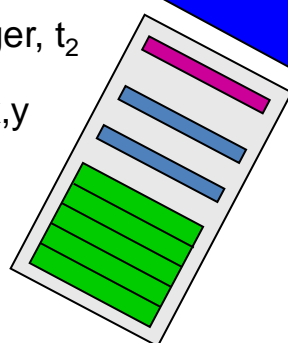


${}^{238}\text{U}, 6.2 \text{ MeV/u}$

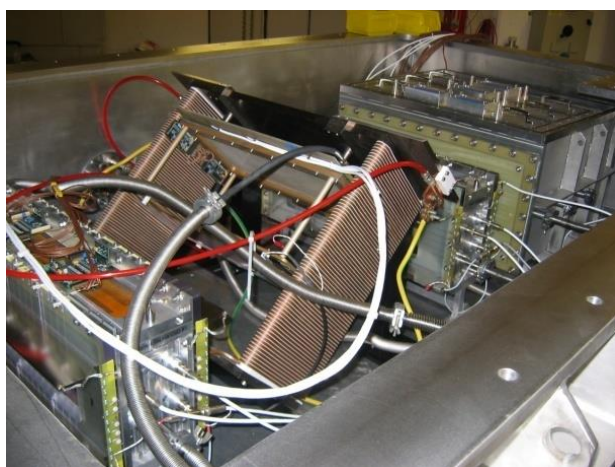
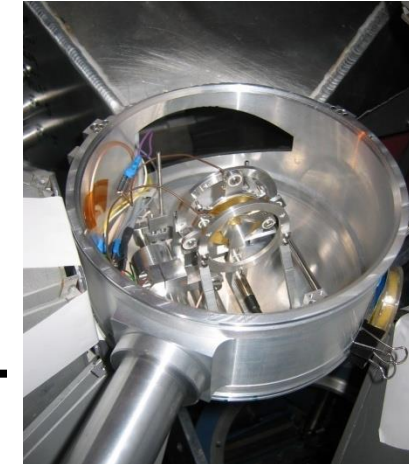
MWPPAC: trigger,  $t_2$

drift chambers: x,y

ionisation  
chamber:  $\Delta E$ , E

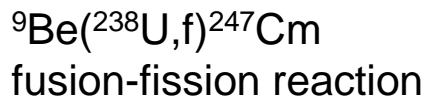


MWPPAC:  $t_1$

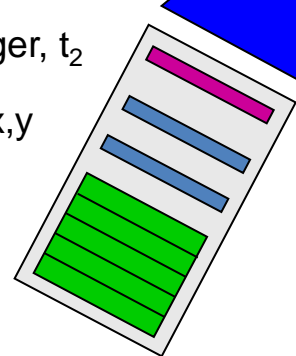


# Heavy-ion induced fission experiments with VAMOS

June 2017



MWPPAC: trigger,  $t_2$   
drift chambers: x,y  
ionisation chamber:  $\Delta E$ , E



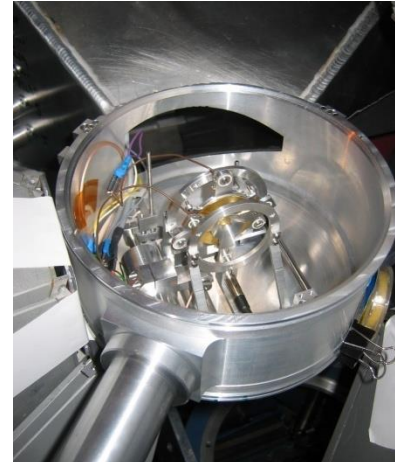
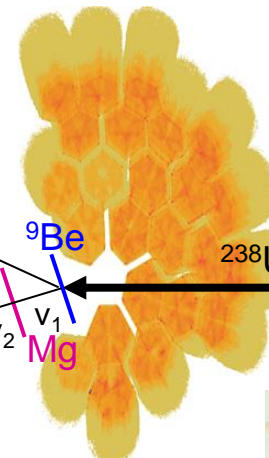
20°

Q

Q

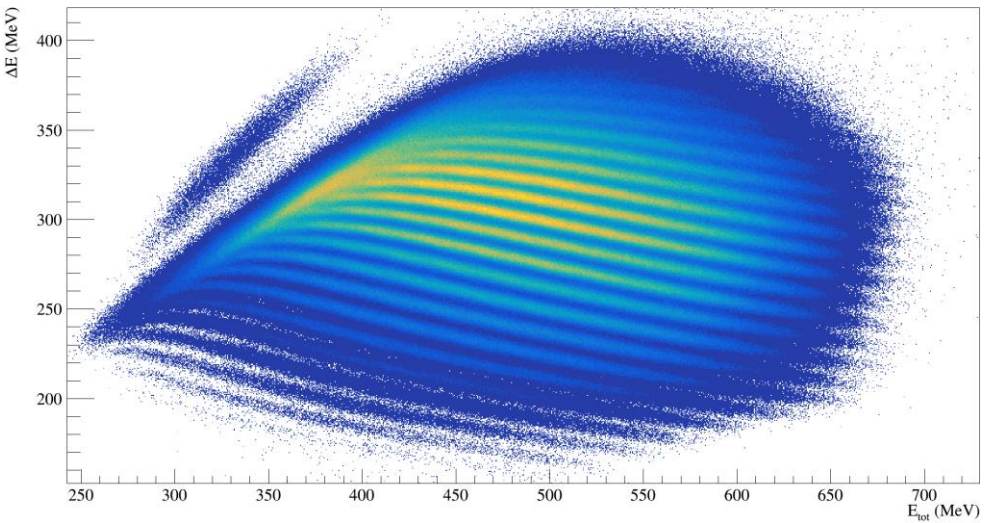
D

MWPPAC:  $t_1$

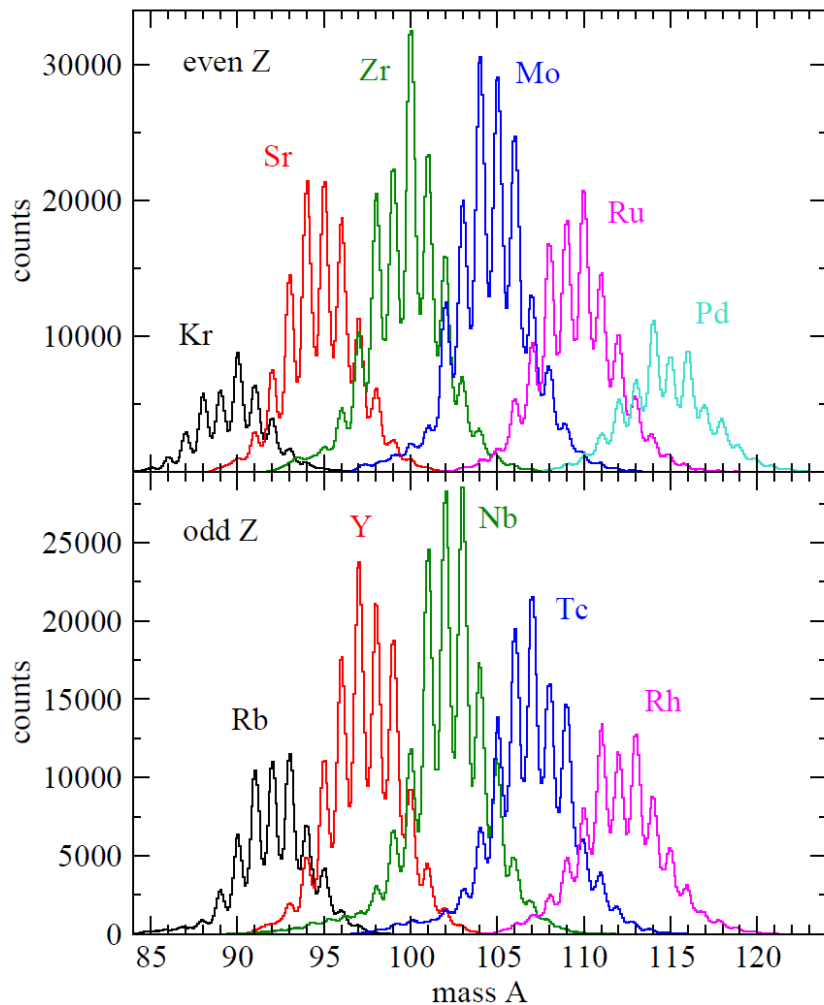
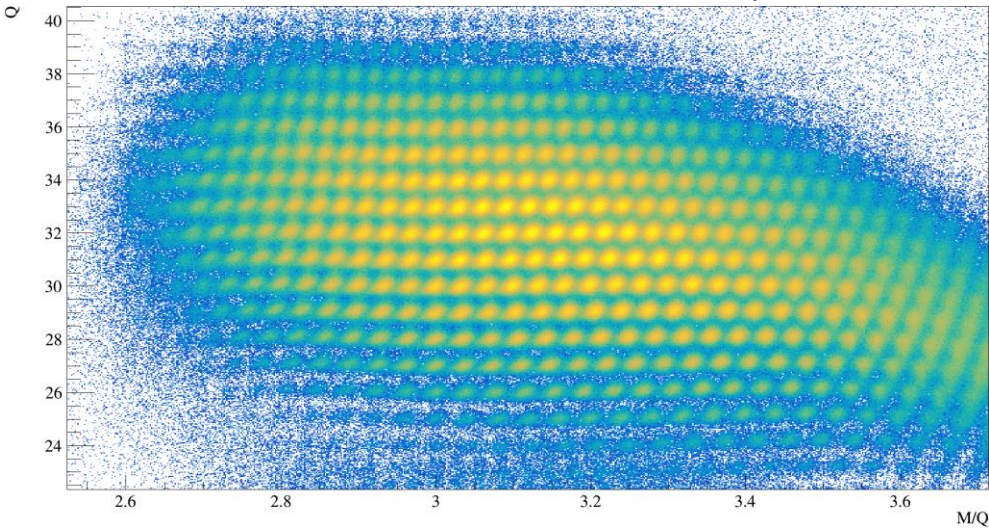


# Identification of fission fragments in VAMOS

energy loss and total energy in ionization chamber  $\Rightarrow Z$

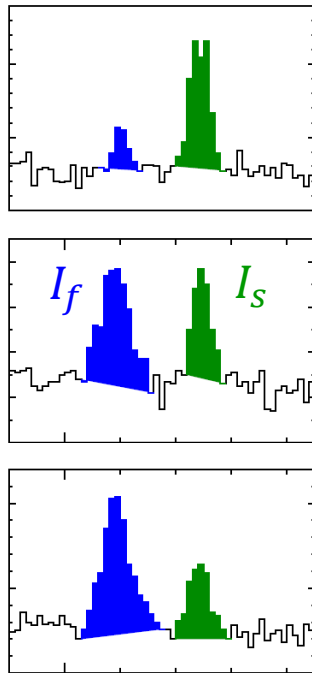
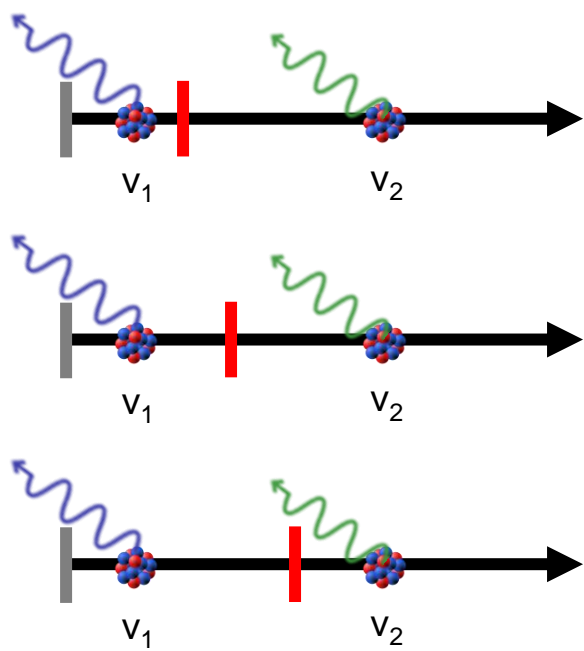


reconstructed trajectory, magnetic rigidity  
time of flight, total energy  $\Rightarrow$  mass  $M$  and  $M/Q$

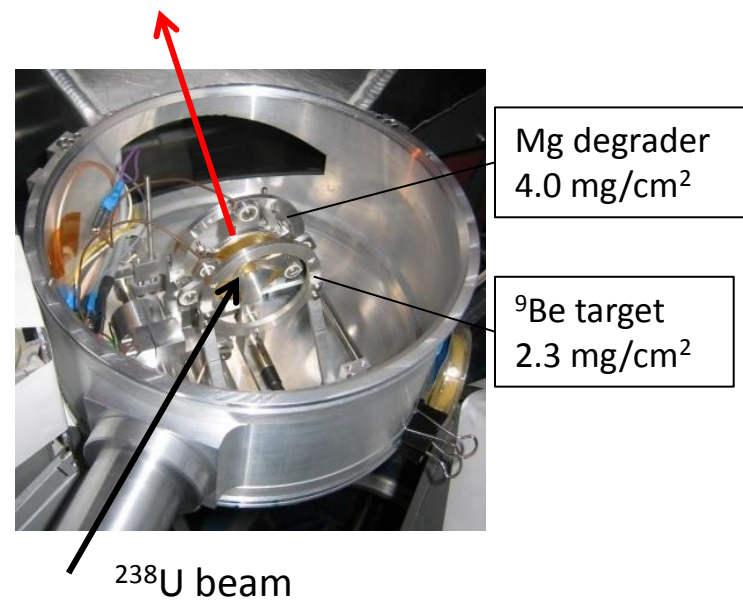


event-by-event identification  
in  $Z$  and  $A$  of more than 200  
fission fragments

# Recoil distance Doppler shift (RDDS) method



fission fragments  
into VAMOS

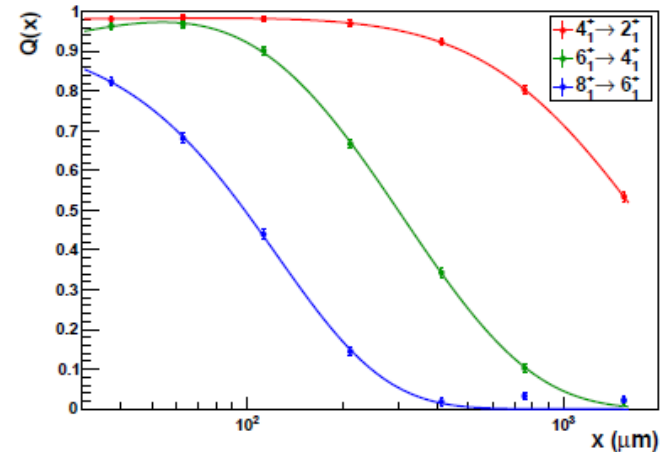
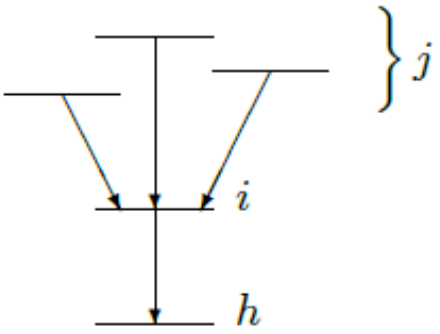


10 distances: 30 – 2650  $\mu\text{m}$   
18 h per distance

decay curve:

$$Q_i(x) = \frac{I_{i,S}(x)}{I_{i,S}(x) + I_{i,F}(x)}$$

$$\tau_i(x) = -\frac{Q_i(x) - \sum_j \alpha_{ij} Q_j(x)}{v_1 \frac{dQ_i}{dx}(x)}$$



A. Dewald et al., Z. Phys. A. 334, 163 (1989)

# Lifetime results in even-even nuclei

$^{112}\text{Pd}$	$^{114}\text{Pd}$	$^{116}\text{Pd}$
2 <sup>+</sup> 84 (14) 4 <sup>+</sup> <b>5.4 (1.7)</b>	2 <sup>+</sup> 82 (14) 4 <sup>+</sup> <b>5.7 (9)</b>	2 <sup>+</sup> 110 (30) 4 <sup>+</sup> <b>8.7 (12)</b> 6 <sup>+</sup> <b>2.6 (9)</b>

Lifetimes in ps

- adopted values
- this work

$^{108}\text{Ru}$	$^{110}\text{Ru}$	$^{112}\text{Ru}$
2 <sup>+</sup> 360 (30) 4 <sup>+</sup> 13.4 (10) <b>13.6 (9)</b> 6 <sup>+</sup> <b>2.9 (3)</b>	2 <sup>+</sup> 320 (20) 4 <sup>+</sup> 15.4 (17) <b>15.1 (9)</b> 6 <sup>+</sup> 2.4 (10) <b>3.2 (5)</b>	2 <sup>+</sup> 320 (30) 4 <sup>+</sup> <b>14.6 (21)</b>

$^{102}\text{Mo}$	$^{104}\text{Mo}$	$^{106}\text{Mo}$	$^{108}\text{Mo}$
2 <sup>+</sup> 125 (4)	2 <sup>+</sup> 970 (80)	2 <sup>+</sup> 1250 (30)	2 <sup>+</sup> 500 (300)
4 <sup>+</sup> 12.5 (25)	4 <sup>+</sup> 26.1 (3)	4 <sup>+</sup> 25.4 (51)	4 <sup>+</sup> <b>23.3 (51)</b>
<b>9.4 (10)</b>	<b>18.6 (9)</b>	<b>28.0 (13)</b>	
6 <sup>+</sup> <b>3.4 (6)</b>	6 <sup>+</sup> 4.73 (15)	6 <sup>+</sup> 4.2 (18)	6 <sup>+</sup> <b>3.1 (3)</b>
	<b>2.8 (2)</b>		

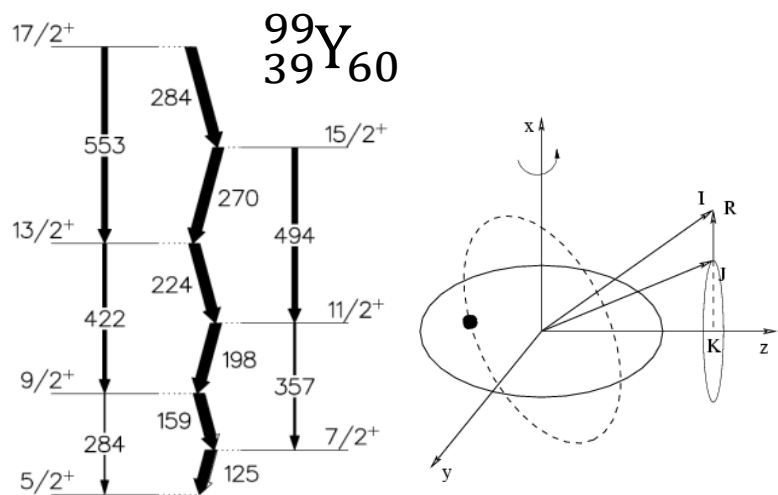
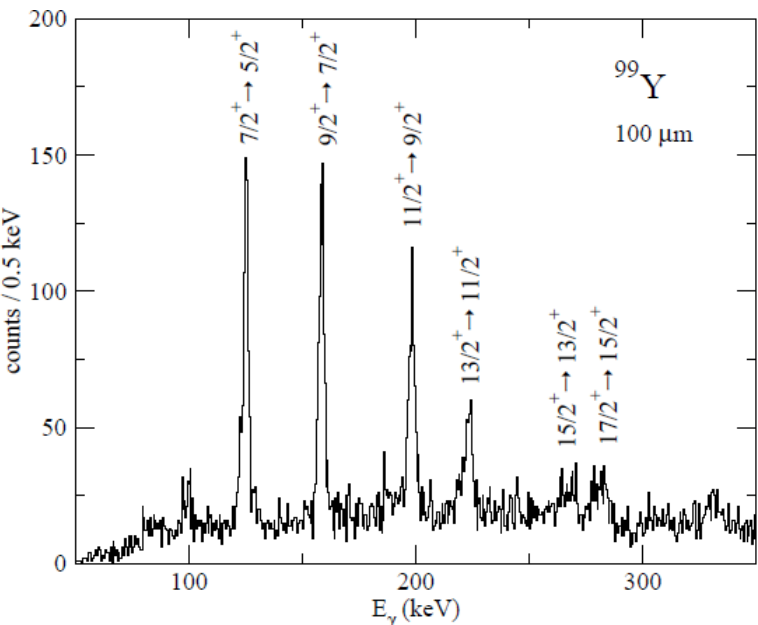
L. Grente, PhD Univ. Paris Sud, 2014  
and to be published

$^{98}\text{Zr}$	$^{100}\text{Zr}$	$^{102}\text{Zr}$
2 <sup>+</sup> <11ps <b>4.9 (26)</b>	2 <sup>+</sup> 590 (30)	2 <sup>+</sup> 1800 (400)
4 <sup>+</sup> 37 (3) <b>18.1 (14)</b>	4 <sup>+</sup> 32.1 (34)	4 <sup>+</sup> <b>4.7 (5)</b>
6 <sup>+</sup> 4.9 (11) <b>3.1 (3)</b>		

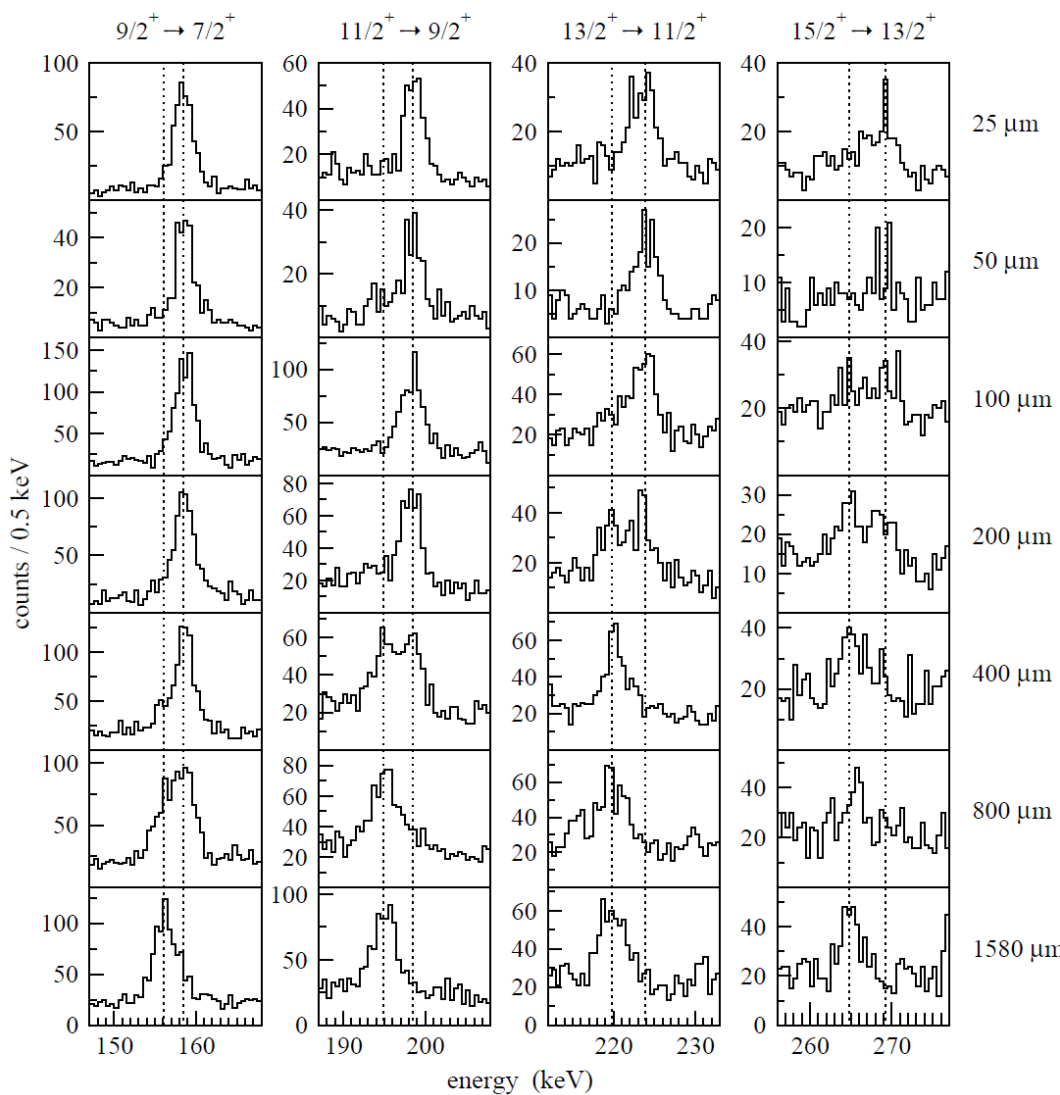
Pd104	Pd105	Pd106	Pd107	Pd108	Pd109	Pd110	Pd111	Pd112	Pd113	Pd114	Pd115	Pd116	Pd117	Pd118	Pd119
0+ 22.33	0+ 27.33	0+ 35.36	6.5E-6 y	0+ 26.46	13.7012 h	0+ 11.72	23.4 m	0+ 11.72	93.5	2.42 m	25.5	11.8	4.3	1.9	0.92
11.14	Rh104	Rh105	Rh106	Rh107	Rh108	Rh109	Rh110	Rh111	Rh112	Rh113	Rh114	Rh115	Rh116	Rh117	Rh118
1/2- *	42.3	1+-	35.36 h	1+-	72+-	21.7 m	6.0 m	31.5	21.5	2.80	1.35	0.99	0.68	0.44	0.26
100	EC, B	B	B	B	B	B	B	B	B	B	B	B	B	B	B
Ru102	Ru103	Ru104	Ru105	Ru106	Ru107	Ru108	Ru109	Ru110	Ru111	Ru112	Ru113	Ru114	Ru115	Ru116	Ru117
0+ 31.6	0+ 39.26 d	0+ 32/-	0+ 18.7	0+ 4.44 h	0+ 37.59 d	0+ 3.75 m	0+ 4.55 m	0+ 14.8	0+ 11.2	0+ 1.75	0+ 0.80	0+ 0.53	0+ 0.40	0+ 0.26	0+ 0.13
B	B	B	B	B	B	B	B	B	B	B	B	B	B	B	B
Tc101	Tc102	Tc103	Tc104	Tc105	Tc106	Tc107	Tc108	Tc109	Tc110	Tc111	Tc112	Tc113	Tc114	Tc115	
14.22 m	5.28 s	54.2 s	18.3 m	7.6 m	35.6 s	21.2 s	5.17 s	0.87 s	0.92 s	0.30 s	0.26 s	130 ms	Tc114	Tc115	
(9/2)+	1+-	*	3/2+	3/2-	3/2-	1/2-	1/2-	1/2-	(1/2+, 2+)	1/2-	1/2-	1/2-	1/2-	1/2-	
B	B	B	B	B	B	B	B	B	B	B	B	B	B	B	
Mo100	Mo101	Mo102	Mo103	Mo104	Mo105	Mo106	Mo107	Mo108	Mo109	Mo110	Mo111	Mo112	Mo113		
1/2, 19/2 y	0+	1/2+	0+	0+	0+	0+	3.5 s	1.09	0.53 s	0.30 s	0.26 s	Tc113	Tc114	Tc115	
B	B	B	B	B	B	B	B	B	B	B	B	B	B	B	
Nb99	Nb100	Nb101	Nb102	Nb103	Nb104	Nb105	Nb106	Nb107	Nb108	Nb109	Nb110	Nb111	Nb112	Nb113	
15.0	1.5	1+-	1+-	1+-	4.8	2.95	1.02	3.80 ms	0.19	0.19	0.17				
9/2+	*	*	*	5/2+	1+-	1+-	1+-	1+-	1+-	1+-	1+-				
B	B	B	B	B	B	B	B	B	B	B	B	B	B	B	
Zr98	Zr99	Zr100	Zr101	Zr102	Zr103	Zr104	Zr105	Zr106	Zr107	Zr108					
30.7	2.1	7.1	1.3	1.3	4.8	1.3	1.3	0+	0+	0+					
0+	(1/2+)	0+	0+	(3/2+)	0+	0+	0+	0+	0+	0+					
B	B	B	B	B	B	B	B	B	B	B	B	B	B	B	

⇒ comparison of B(E2) values  
with beyond-mean field calculations

# Lifetime measurement for odd-mass Y isotopes with EXOGAM

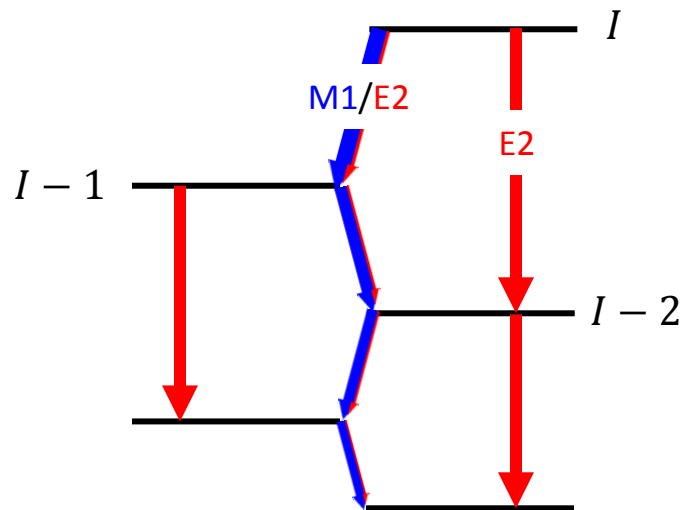


deformed  $^{98}\text{Sr}$  plus extra proton  
 $\Rightarrow$  strongly coupled band



T.W.Hagen et al.,  
PRC 95, 034302 (2017)

## Rotational bands in the particle – rotor model



branching ratio:  $\frac{I_\gamma(\Delta I = 1)}{I_\gamma(\Delta I = 2)} \Rightarrow \frac{B(M1)}{B(E2)}$

lifetime:  $\frac{1}{\tau} = \lambda_{tot} = \lambda_{M1} + \lambda_{E2,\Delta I=1} + \lambda_{E2,\Delta I=2}$

$\Rightarrow$  absolute  $B(M1)$  and  $B(E2)$  values

$\Rightarrow$  comparison with theoretical calculations

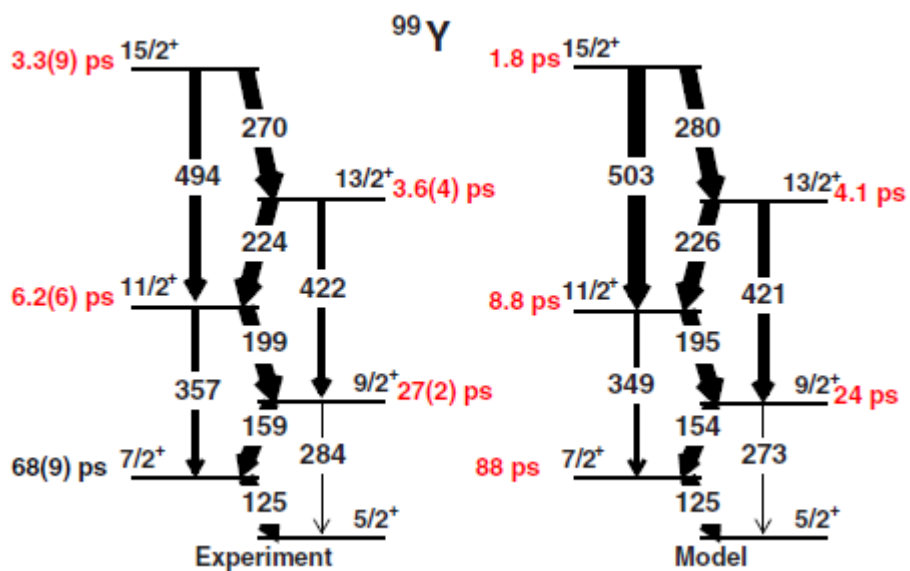
Particle – rotor model:  $B(M1; I_i K \rightarrow I_f K) = \frac{3}{4\pi} e^2 (g_K - g_R)^2 K^2 |\langle I_i 1K0 | I_f K \rangle|^2$

$$B(E2; I_i K \rightarrow I_f K) = \frac{5}{16\pi} e^2 Q_0^2 |\langle I_i 2K0 | I_f K \rangle|^2$$

branching ratio:  $\frac{B(M1)}{B(E2)} \Rightarrow \frac{(g_K - g_R)}{Q_0}$

- lifetime:
- $(g_K - g_R) \Rightarrow$  configuration of the odd particle
  - $Q_0 \Rightarrow$  deformation of the core

## Results for $^{99}\text{Y}$



microscopic particle-rotor calculations  
with  $\varepsilon_2 = 0.41$  and  $\gamma = 0^\circ$

T.W.Hagen et al.,  
PRC 95, 034302 (2017)

$I_i$	$b_{E2/M1}$	$\tau$ [ps]	$g_K - g_R$	$Q_0$ [eb]
9/2	0.18	27	0.97	5.0
11/2	0.35	6.2	1.25	5.9
13/2	0.45	3.6	1.27	5.0
15/2	0.64	3.3	0.92	3.7

### Laser spectroscopy of $5/2^+$ ground state

B. Cheal et al., Phys. Lett. B 645, 133 (2007)

➤  $\mu = 3.18(2) \mu_N$

with  $g_R = Z/A \Rightarrow (g_K - g_R) = 1.23$

consistent with [422]5/2<sup>+</sup> configuration

➤  $Q_s = +1.55(17) \text{ eb}$

rotational model:  $Q_s = \frac{3K^2 - I(I+1)}{(I+1)(2I+3)} Q_0$

⇒  $Q_0 = 4.34(48) \text{ eb}$

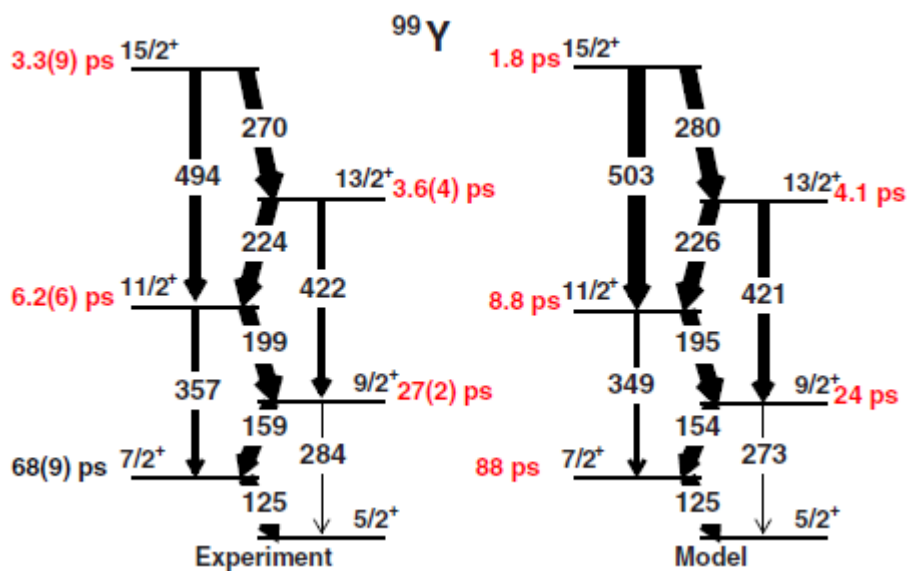
### Coulomb excitation of $^{98}\text{Sr}$ :

E. Clément et al., PRL 116, 022701 (2016)

➤  $Q_s(4^+) = -1.87^{+14}_{-25} \text{ eb}$

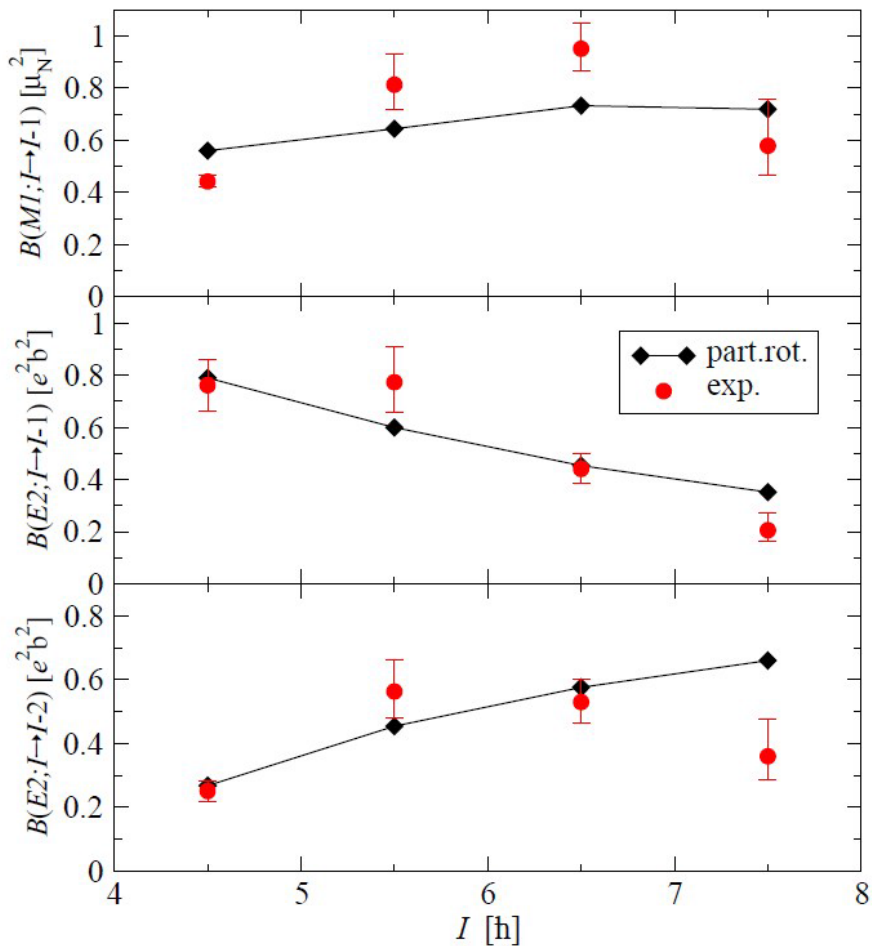
⇒  $Q_0 = 5.14^{+0.39}_{-0.69} \text{ eb}$

## Results for $^{99}\text{Y}$

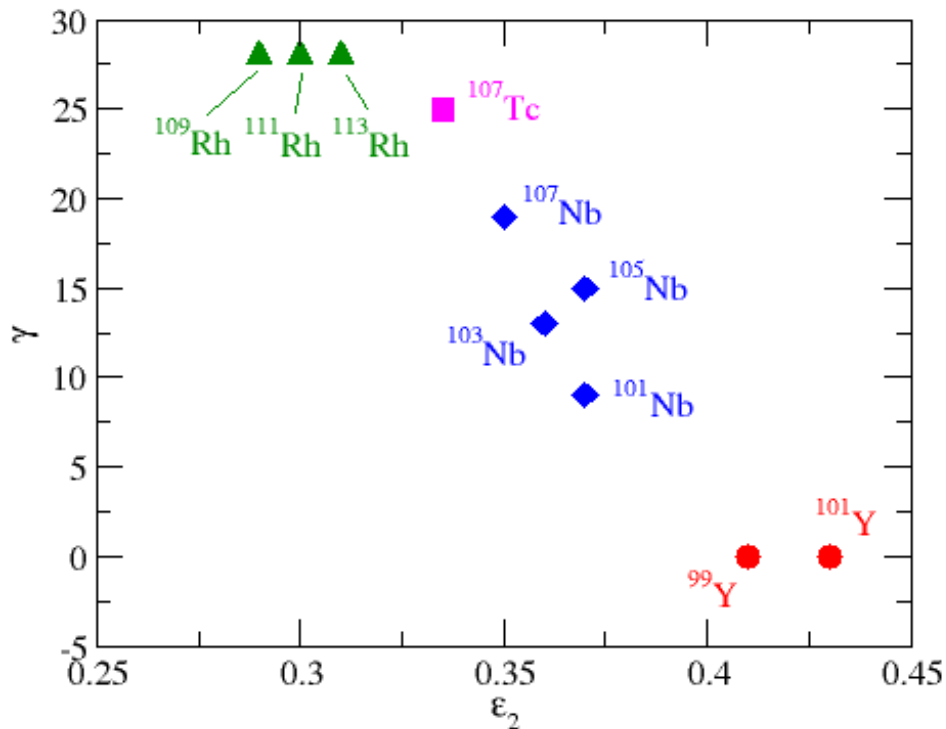
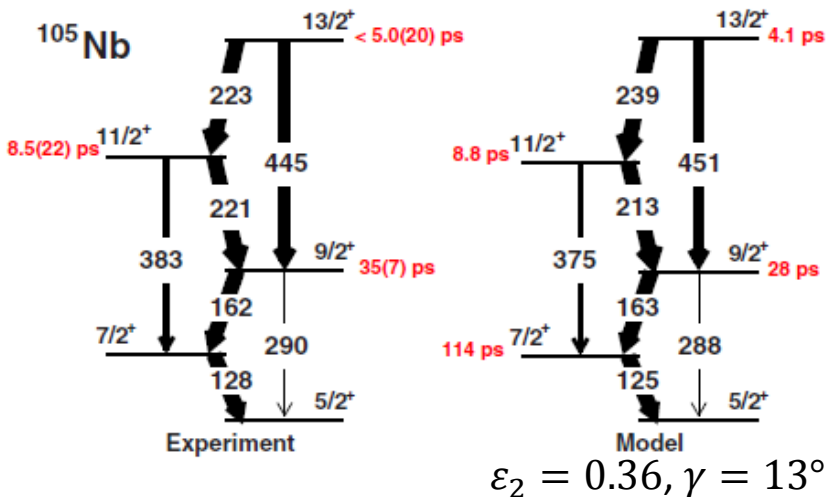


microscopic particle-rotor calculations  
with  $\varepsilon_2 = 0.41$  and  $\gamma = 0^\circ$

T.W.Hagen et al.,  
PRC 95, 034302 (2017)



# Many more results from the same experiment

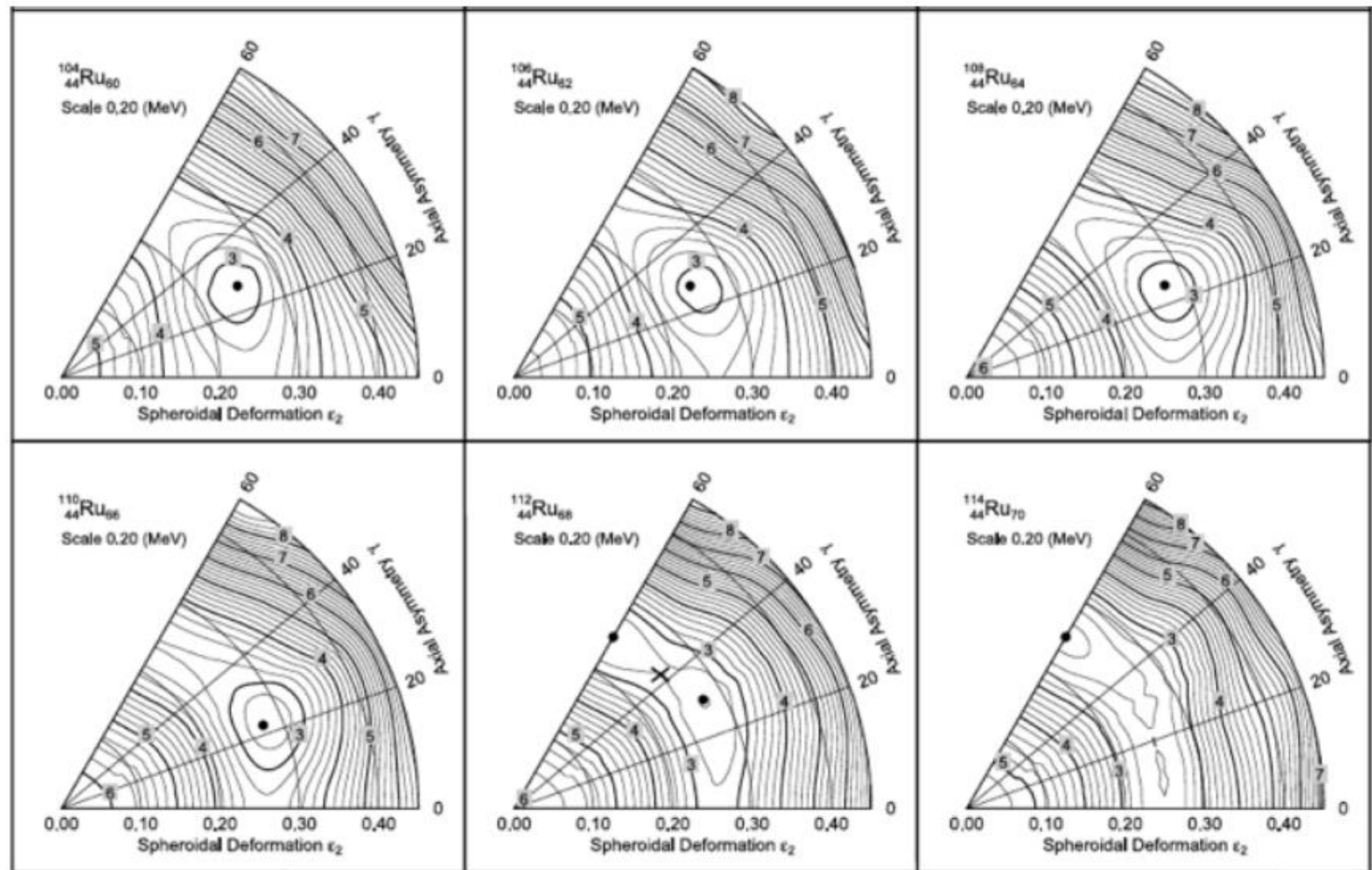


Results for  $^{39}\text{Y}$ ,  $^{41}\text{Nb}$ ,  $^{43}\text{Tc}$ ,  $^{45}\text{Rh}$ :  
with increasing  $Z$ :  
 ➤ increase of triaxiality  $\gamma$   
 ➤ decrease of deformation  $\varepsilon_2$

54	Ru95 5.02 m (9/2) <sup>-</sup>	Ru96 9.90 m 6+	Ru96 30.7 m (9/2) <sup>-</sup>	Ru95 8.7 m (2) <sup>-</sup>	Ru99 16.1 d 1/2 <sup>+</sup>	Ru100 20.8 h 1-	Ru101 3.3 y 1/2 <sup>+</sup>	Ru102 207.4 (3-2)	Ru103 10.1	Ru104 42.3 s 1+	Ru105 35.34 h 7/2 <sup>+</sup>	Ru106 29.90 s 1+	Ru107 21.7 m 7/2 <sup>+</sup>	Ru108 6.9 m (5/2) <sup>-</sup>	Ru109 90 s 7/2 <sup>+</sup>	Ru110 3.2 s 1+	Ru111 11 s (7/2) <sup>-</sup>	Ru112 2.1 s 1+	Ru113 2.00 s 1+	Ru114 1.95 s 1+	Ru115 0.99 s (7/2) <sup>-</sup>	Ru116 0.68 s 1+	Ru117 0.44 s (7/2) <sup>-</sup>	Ru118	Ru119	Ru120	Ru121					
53	Ru94 5.18 m 6-	Ru95 1.45 d 5/2 <sup>+</sup>	Ru96 9+	Ru97 2.9 d 5/2 <sup>+</sup>	Ru98 9+	Ru99 5.2 s	Ru100 9+	Ru101 5.2 s	Ru102 9+	Ru103 39.25 d 3/2 <sup>-</sup>	Ru104 37.539 s 3/2 <sup>-</sup>	Ru105 4.44 s 3/2 <sup>-</sup>	Ru106 37.539 s 3/2 <sup>-</sup>	Ru107 3.75 m (5/2) <sup>-</sup>	Ru108 4.55 m (5/2) <sup>-</sup>	Ru109 34.5 s (5/2) <sup>-</sup>	Ru110 14.6 s 3/2 <sup>-</sup>	Ru111 2.12 s 3/2 <sup>-</sup>	Ru112 1.75 s 3/2 <sup>-</sup>	Ru113 0.80 s 3/2 <sup>-</sup>	Ru114 0.53 s 3/2 <sup>-</sup>	Ru115 0.40 s 3/2 <sup>-</sup>	Ru116 0 s 3/2 <sup>-</sup>	Ru117 0 s 3/2 <sup>-</sup>	Ru118							
52	Tc93 2.75 h 9/2 <sup>+</sup>	Tc94 2.93 m 7+	Tc95 20.0 h 9/2 <sup>+</sup>	Tc96 4.28 d 5/2 <sup>+</sup>	Tc97 2.616 y 9/2 <sup>+</sup>	Tc98 4.23 d 9/2 <sup>+</sup>	Tc99 1.88	Tc100 12.7	Tc101 12.6	Tc102 17.9	Tc103 31.6	Tc104 14.22 d (3/2) <sup>-</sup>	Tc105 2.58 s 3/2 <sup>-</sup>	Tc106 4.44 s 3/2 <sup>-</sup>	Tc107 3.75 m (5/2) <sup>-</sup>	Tc108 4.55 m (5/2) <sup>-</sup>	Tc109 34.5 s (5/2) <sup>-</sup>	Tc110 5.17 s (3/2) <sup>-</sup>	Tc111 0.97 s 3/2 <sup>-</sup>	Tc112 0.92 s (3/2) <sup>-</sup>	Tc113 0.80 s 3/2 <sup>-</sup>	Tc114 0.53 s 3/2 <sup>-</sup>	Tc115 0.40 s 3/2 <sup>-</sup>	Tc116 0 s 3/2 <sup>-</sup>	Tc117 0 s 3/2 <sup>-</sup>	Tc118						
51	Mn92 4.08 d 5/2 <sup>+</sup>	Mn93 4.08 d 5/2 <sup>+</sup>	Mn94 9+	Mn95 9+	Mn96 9+	Mn97 9+	Mn98 9+	Mn99 6.94 s 1/2 <sup>+</sup>	Mn100 1.93 d 9/2 <sup>+</sup>	Mn101 14.61 s 1/2 <sup>+</sup>	Mn102 11.3 s 1/2 <sup>+</sup>	Mn103 6.75 s (3/2) <sup>-</sup>	Mn104 6.6 s (3/2) <sup>-</sup>	Mn105 35.6 s 1/2 <sup>+</sup>	Mn106 4.4 s 1/2 <sup>+</sup>	Mn107 6.6 s 1/2 <sup>+</sup>	Mn108 1.09 s 9+	Mn109 0.85 s 9+	Mn110 0.53 s 9+	Mn111 0 s 9+	Mn112 0 s 9+	Mn113 0 s 9+	Mn114 0 s 9+	Mn115 0 s 9+	Mn116 0 s 9+	Mn117 0 s 9+	Mn118					
50	Nb91 6.69 y 3/2 <sup>+</sup>	Nb92 3.476+7 y (7/2) <sup>-</sup>	Nb93 2.038+4 y (9/2) <sup>-</sup>	Nb94 34.975 d 9/2 <sup>+</sup>	Nb95 23.35 h 9/2 <sup>+</sup>	Nb96 72.1 m 9/2 <sup>+</sup>	Nb97 2.96 s 1+	Nb98 15.9 s 1+	Nb99 1.5 s 1+	Nb100 7.1 s 1+	Nb101 7.1 s 1+	Nb102 1.5 s 1+	Nb103 1.5 s (5/2) <sup>-</sup>	Nb104 4.8 s (3/2) <sup>-</sup>	Nb105 2.95 s (3/2) <sup>-</sup>	Nb106 1.62 s 1+	Nb107 330 ms (3/2) <sup>-</sup>	Nb108 0.19 s (2)	Nb109 0.19 s (2)	Nb110 0.17 s (2)	Nb111 0 s 1+	Nb112 0 s 1+	Nb113 0 s 1+	Nb114 0 s 1+	Nb115 0 s 1+	Nb116 0 s 1+	Nb117 0 s 1+	Nb118				
49	Zr90 1 h	Zr91 9+	Zr92 9+	Zr93 1.526+4 y 5/2 <sup>+</sup>	Zr94 64.02 d 5/2 <sup>+</sup>	Zr95 16.91 h 5/2 <sup>+</sup>	Zr96 3.67 s 9+	Zr97 2.1 s (1/2) <sup>-</sup>	Zr98 2.1 s (1/2) <sup>-</sup>	Zr99 7.1 s (1/2) <sup>-</sup>	Zr100 2.1 s (1/2) <sup>-</sup>	Zr101 7.1 s (1/2) <sup>-</sup>	Zr102 2.9 s (3/2) <sup>-</sup>	Zr103 1.3 s (5/2) <sup>-</sup>	Zr104 1.2 s (5/2) <sup>-</sup>	Zr105 0.6 s 1+	Zr106 1.09 s 9+	Zr107 0 s 9+	Zr108 0 s 9+	Zr109 0 s 9+	Zr110 0 s 9+	Zr111 0 s 9+	Zr112 0 s 9+	Zr113 0 s 9+	Zr114 0 s 9+	Zr115 0 s 9+	Zr116 0 s 9+	Zr117 0 s 9+	Zr118			
48	Y93 1.64 s 2-	Y94 65.51 d 1/2 <sup>+</sup>	Y95 3.54 s 2-	Y96 10.18 s 2-	Y97 18.7 m 1/2 <sup>+</sup>	Y98 10.3 m 1/2 <sup>+</sup>	Y99 5.54 s 9-	Y99 3.75 s 9-	Y99 0.58 s 9-	Y100 1.470 s 440 ms (5/2) <sup>-</sup>	Y100 7.25 ms 1-3	Y101 1.7 s 1-3	Y102 1.2 s (5/2) <sup>-</sup>	Y103 0.36 s 1-	Y104 0.23 s 1-	Y105 0.19 s 1-	Y106 0 s 1-	Y107 0 s 1-	Y108 0 s 1-	Y109 0 s 1-	Y110 0 s 1-	Y111 0 s 1-	Y112 0 s 1-	Y113 0 s 1-	Y114 0 s 1-	Y115 0 s 1-	Y116 0 s 1-	Y117 0 s 1-	Y118			
47	Sr88 9+	Sr89 56.53 d 5/2 <sup>+</sup>	Sr90 28.79 y 9+	Sr91 0.63 s 5/2 <sup>+</sup>	Sr92 2.71 h 9+	Sr93 7.423 m 9+	Sr94 75.5 s 9+	Sr95 23.90 s 1/2 <sup>+</sup>	Sr96 1.97 s 9+	Sr97 425 ms 9+	Sr98 0.853 s 9+	Sr99 0.209 s 9+	Sr100 202 ms 9+	Sr101 110 ms (5/2) <sup>-</sup>	Sr102 69 ms 9+	Sr103 51 ms 9+	Sr104 9 s 9+															

T.W. Hagen  
PhD Univ. Oslo (2016)

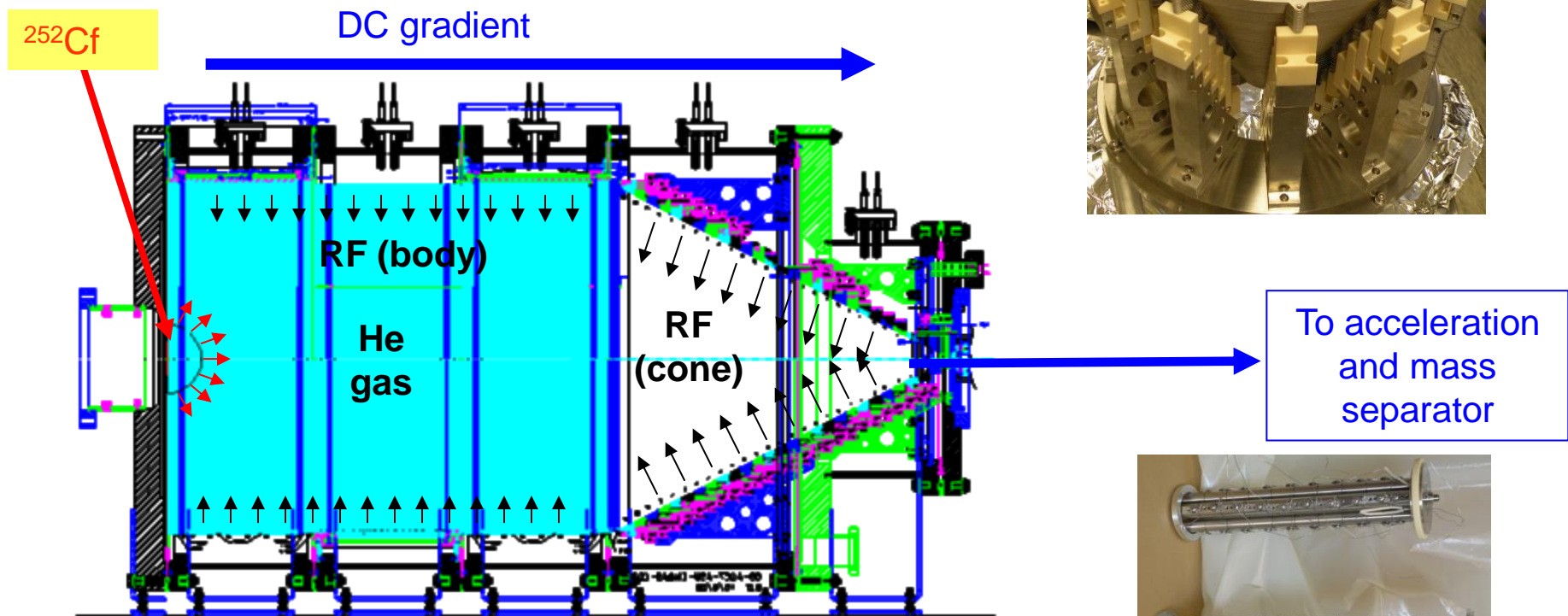
## Triaxiality predicted for $Z \approx 44$ and $N \approx 64$



P. Möller et al., At. Data Nucl. Data Table 94 (2008)

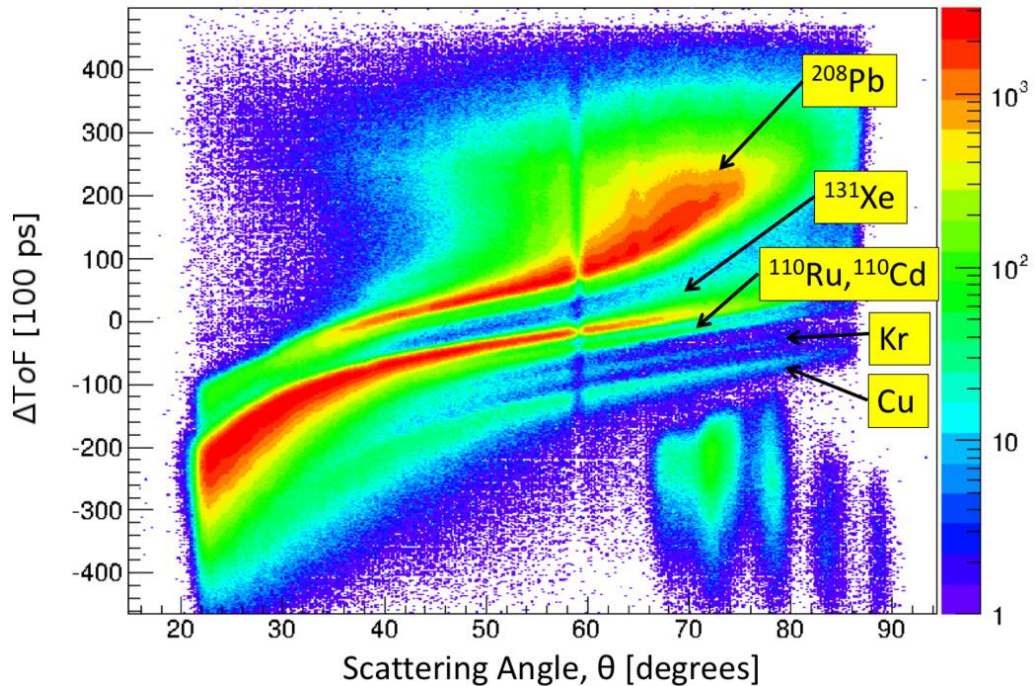
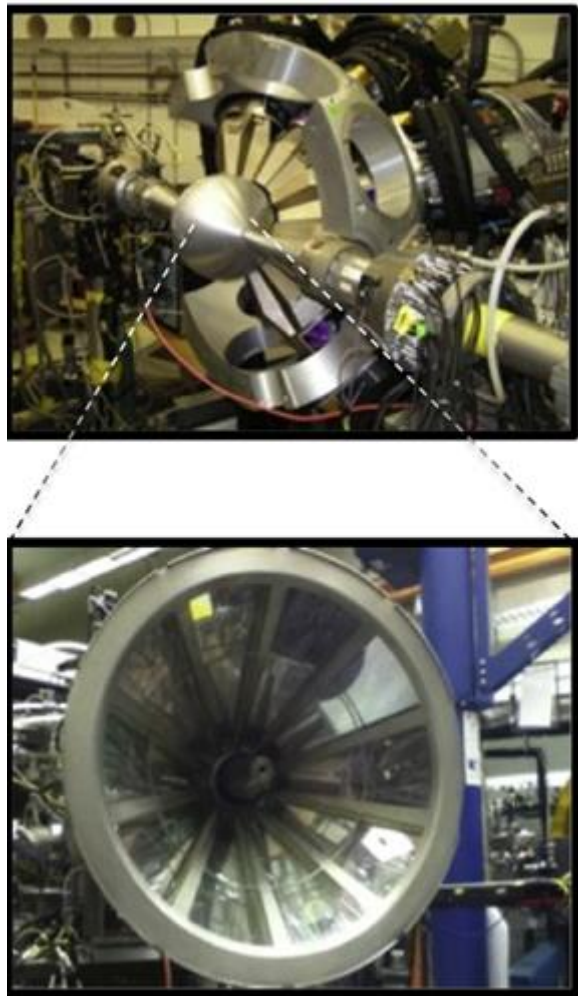
# CARIBU (CALifornium Rare Isotope Breeder Upgrade) at Argonne

- 1.7 Ci  $^{252}\text{Cf}$  source
- recoiling fission fragments stopped in Helium gas
- ion transport by RF field + DC field + gas flow
- Fast and independent of chemistry
- Extraction in 2 RFQ sections



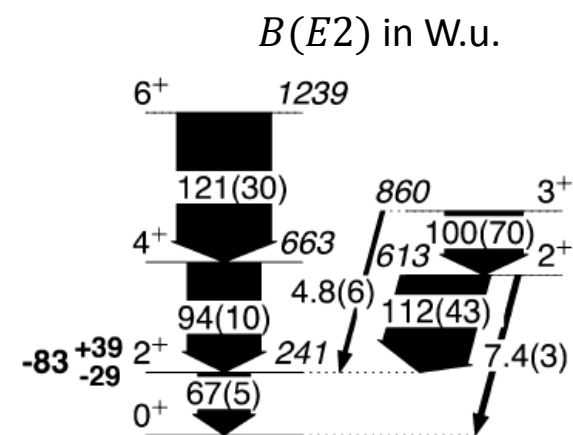
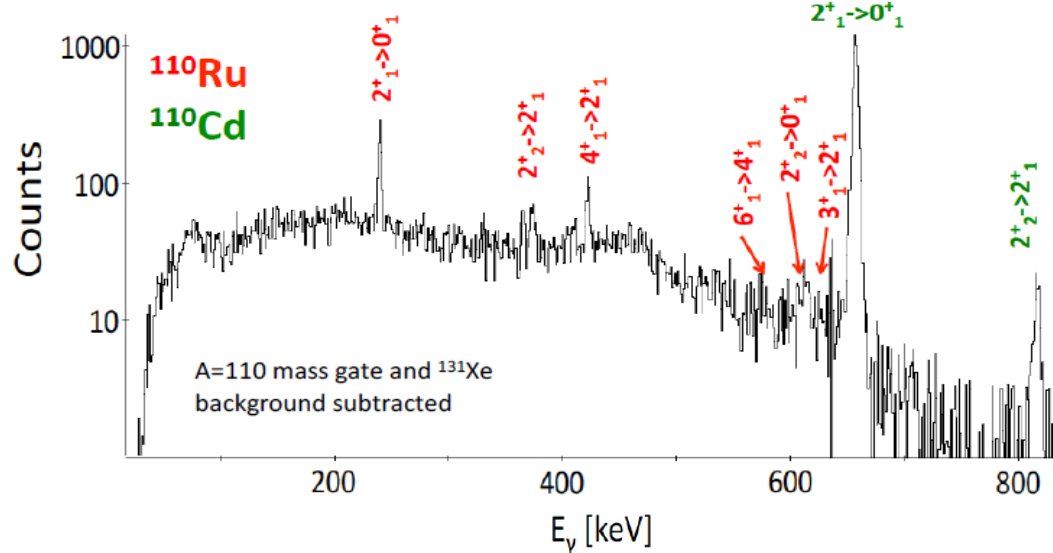
G.Savard et al., Nucl. Instr. Meth. B 266, 4086 (2008)

# Coulomb excitation of $^{110}\text{Ru}$ with GRETINA and CHICO2



- ToF in CHICO2:
  - ⇒ some mass identification:  $\frac{\Delta A}{A} \approx 10\%$
- position resolution in GRETINA and CHICO2:
  - ⇒ Doppler correction
- isobaric contaminants problematic

# Coulomb excitation of $^{110}\text{Ru}$ with GRETINA and CHICO2



D.Doherty et al.,  
Phys.Lett.B 766, 334 (2017)

$\gamma$	$\frac{\epsilon_1(2)}{\epsilon_1(2)}$	$b(E2; 22 \rightarrow 0)$	$b(E2; 22 \rightarrow 21)$	$\frac{b(E2; 22 \rightarrow 21)}{b(E2; 22 \rightarrow 0)}$
0	$\infty$	0	0	1.43
5	64.2	0.0074	0.011	1.49
10	15.9	0.028	0.051	1.70
15	6.85	0.053	0.143	2.70
20	3.73	0.067	0.357	5.35
22.5	2.93	0.0625	0.563	19.02
24	2.59	0.052	0.782	15.1
25	2.41	0.0425	0.865	20.6
26	2.26	0.0324	1.01	31.2
28	2.07	0.010	1.28	126
29	2.01	0.004	1.41	363
30	2.00	0	1.43	$\infty$

$$\frac{E(2^+_2)}{E(2^+_1)} = 2.54$$

$$\frac{B(E2; 2^+_2 \rightarrow 0^+_1)}{B(E2; 2^+_1 \rightarrow 0^+_1)} = 0.11(1)$$

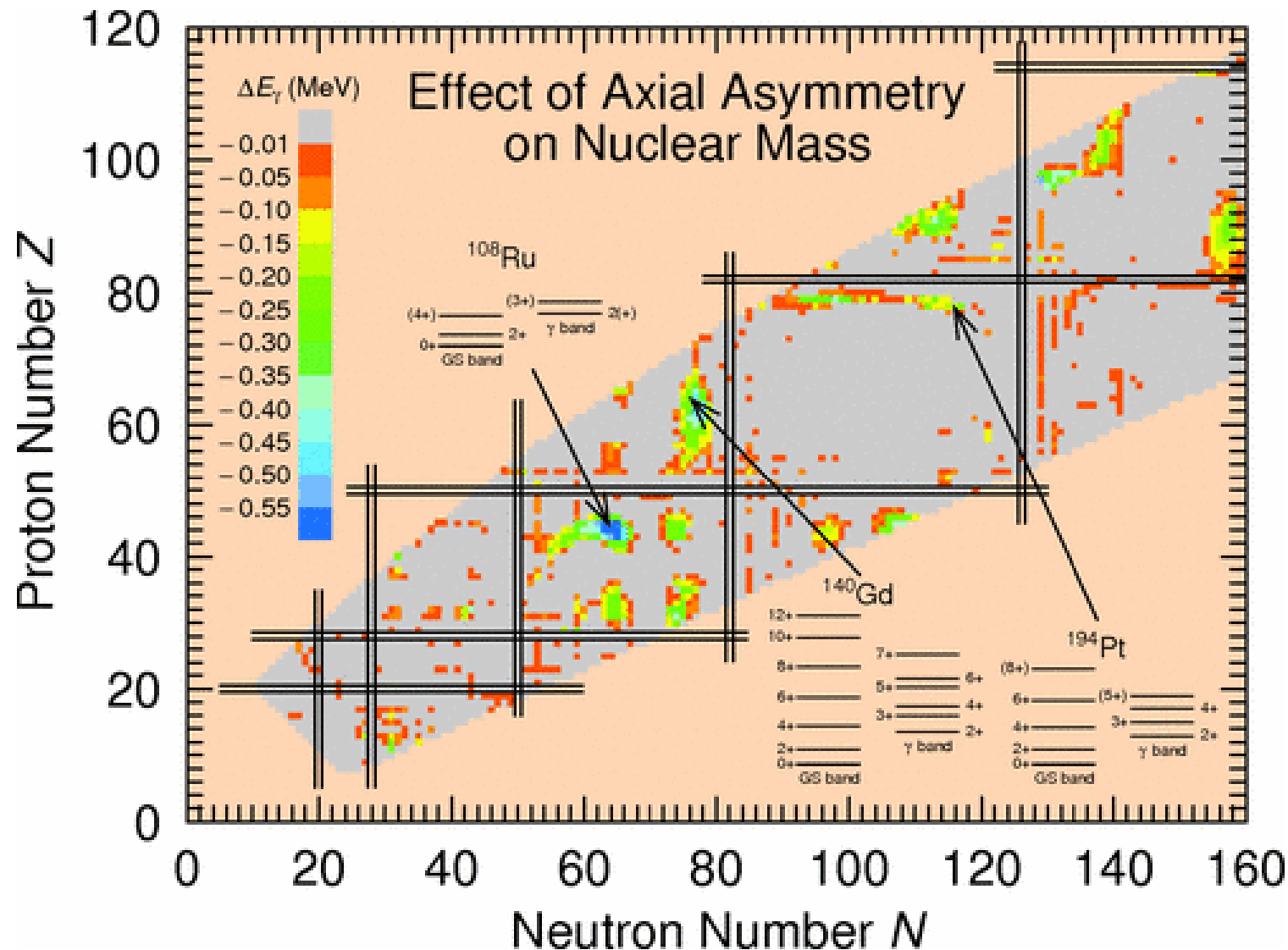
$$\frac{B(E2; 2^+_2 \rightarrow 2^+_1)}{B(E2; 2^+_1 \rightarrow 0^+_1)} = 1.67(65)$$

$$\frac{B(E2; 2^+_2 \rightarrow 2^+_1)}{B(E2; 2^+_2 \rightarrow 0^+_1)} = 15(6)$$

A.S.Davydov and G.F.Filippov, Nucl. Phys. 8, 237 (1958)

$B(E2)$  values compatible with  $\gamma \approx 25^\circ$

# Regions of triaxiality near the ground state

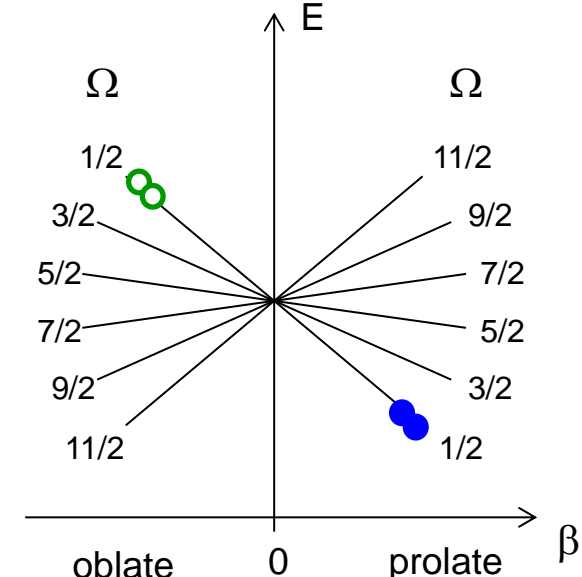
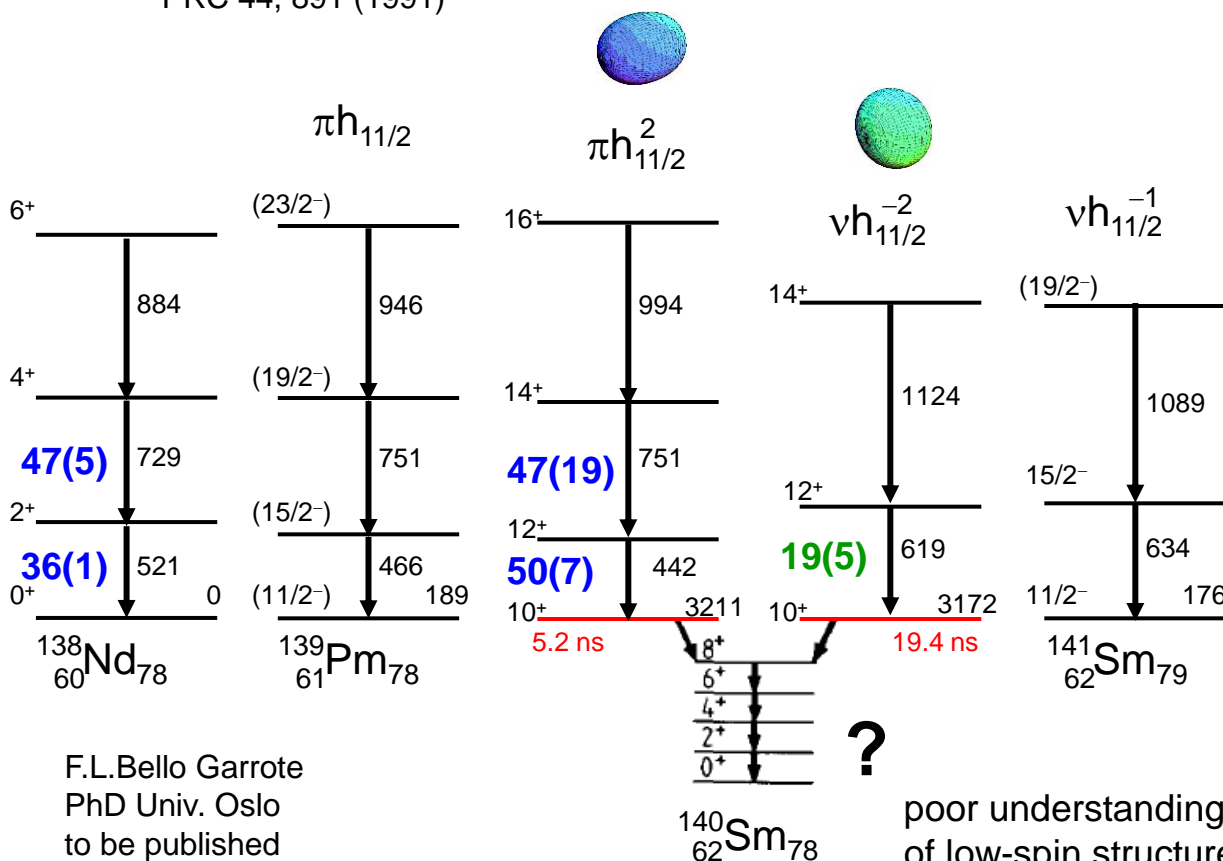


P. Möller et al., Phys. Rev. Lett. 97, 162502 (2006)

# Shape coexistence in $^{140}\text{Sm}$

**B(E2) [W.u.]**

M.A. Cardona et al.  
PRC 44, 891 (1991)



rotationally aligned 2qp bands  
built on  $\pi(h_{11/2})^2$  and  $\nu(h_{11/2})^{-2}$

indirect evidence for  
shape coexistence  
at intermediate spins

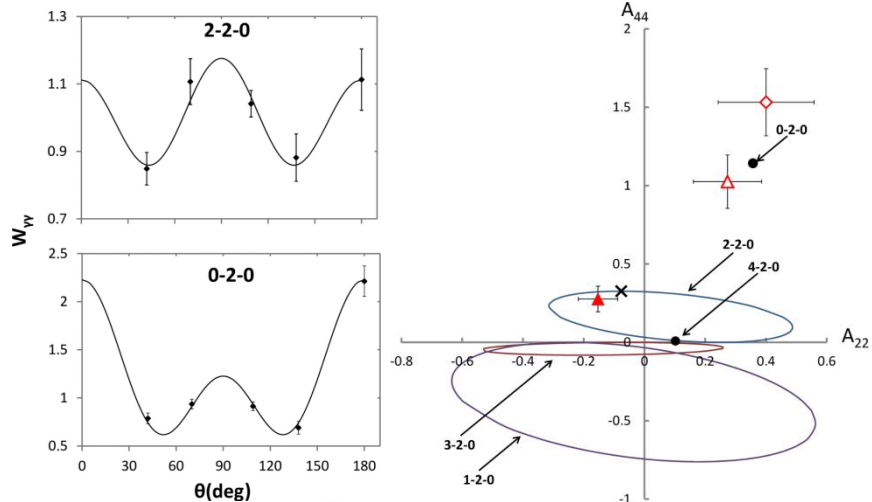
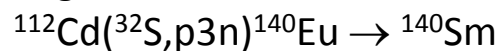
**need B(E2) and Q<sub>s</sub>**

⇒ Coulomb excitation

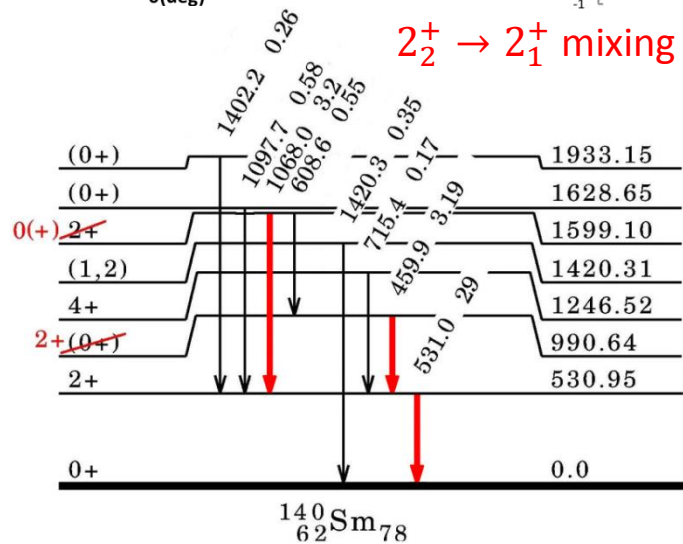
F.L.Bello Garrote  
PhD Univ. Oslo  
to be published

# Shape coexistence also at low spin?

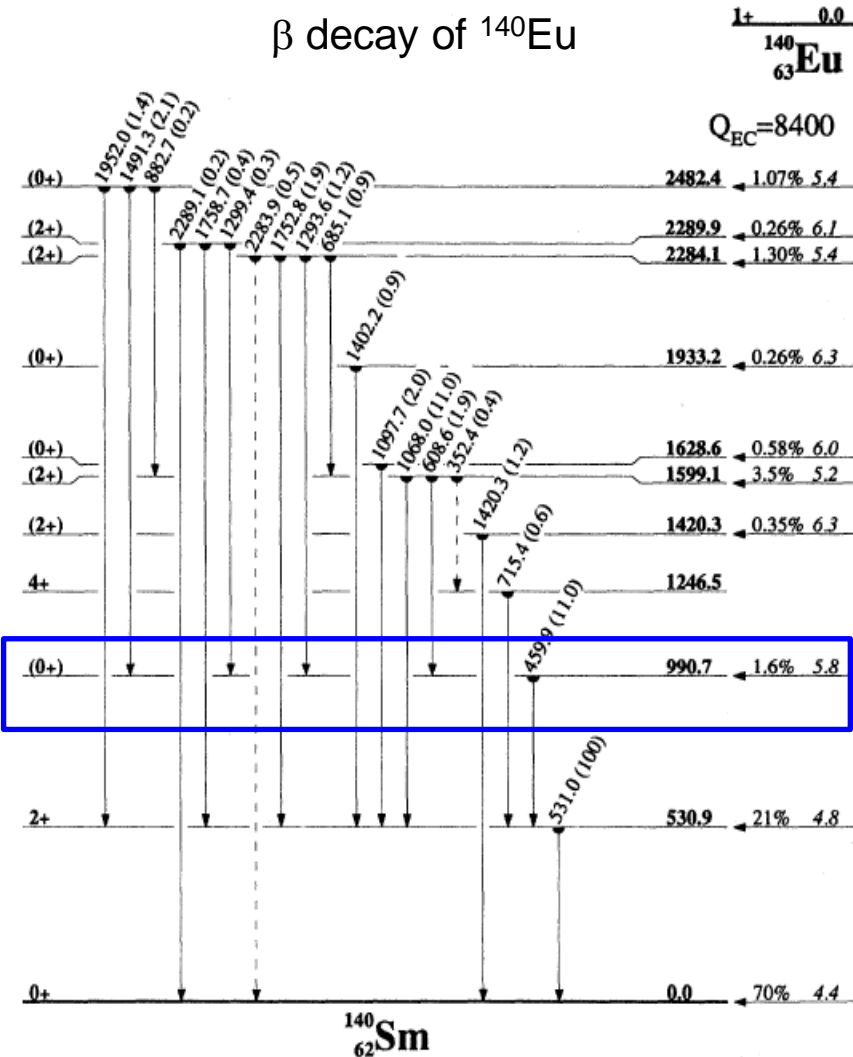
angular correlation measurement



$2_2^+ \rightarrow 2_1^+$  mixing ratio: 98% E2



J.Samorajczyk et al., PRC 92, 044322 (2015)

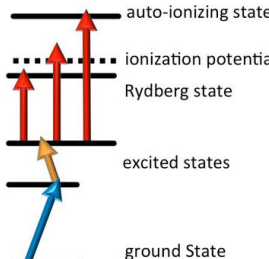
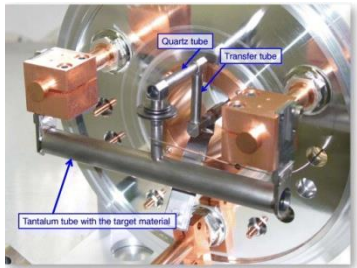
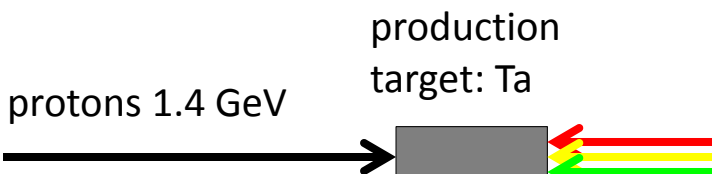


R.B. Firestone et. al.  
PRC 43, 1066 (1991)

low-lying ( $0^+$ ) state ?

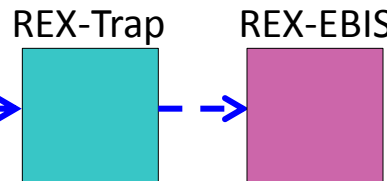
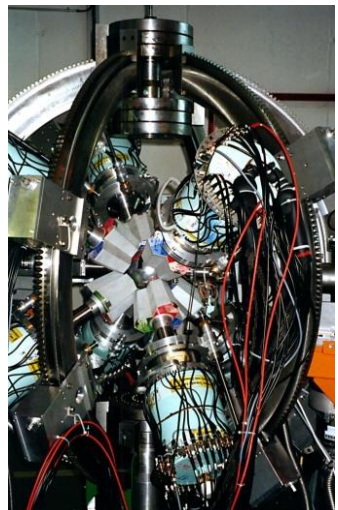
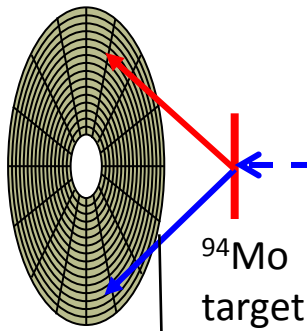
# Isotope separation on-line and postacceleration at ISOLDE

resonant laser ionization

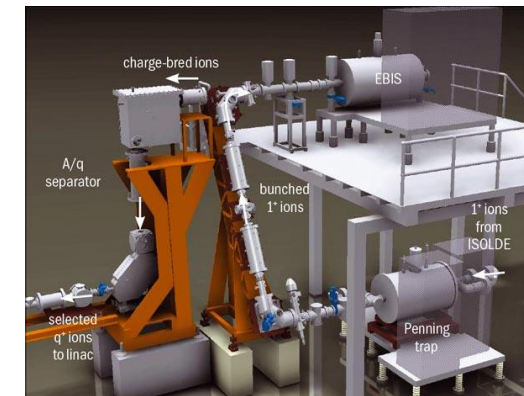


high-resolution mass separator  
 $A = 140$

DSSD

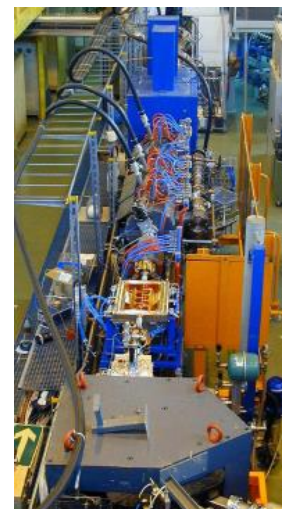


$^{140}\text{Sm}^{29+}$

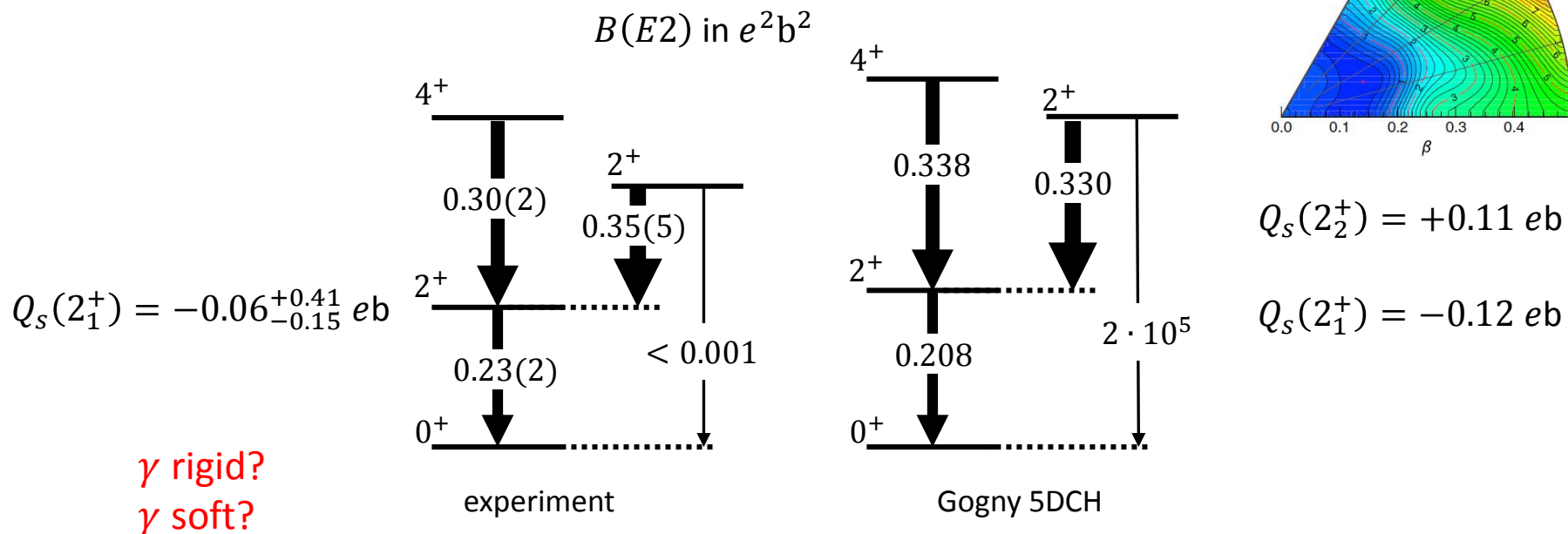
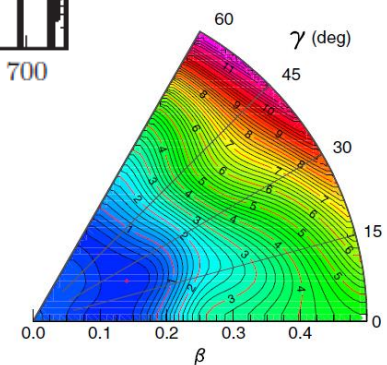
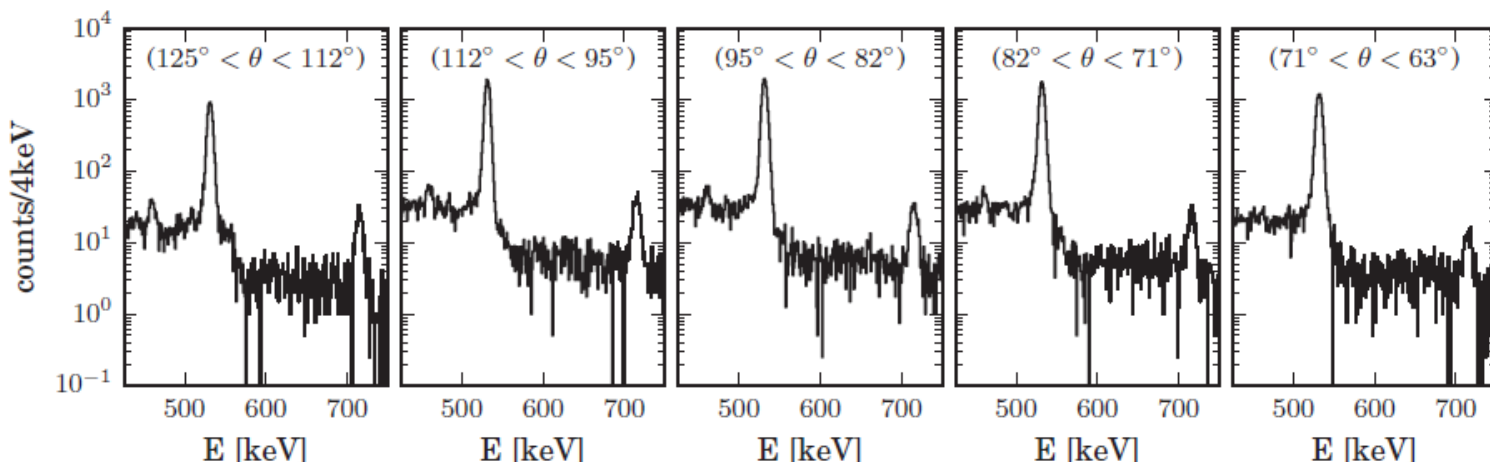


mass separator

Miniball  
Ge detectors



# Coulomb excitation of $^{140}\text{Sm}$

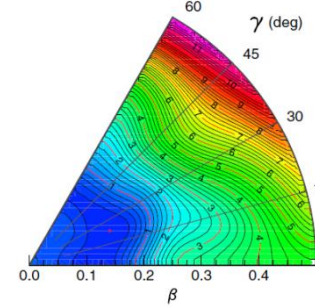
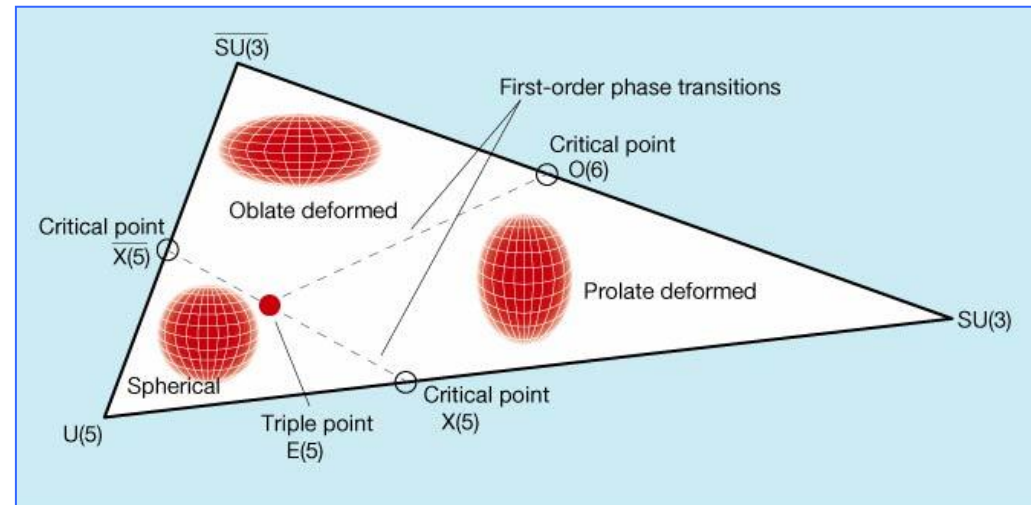
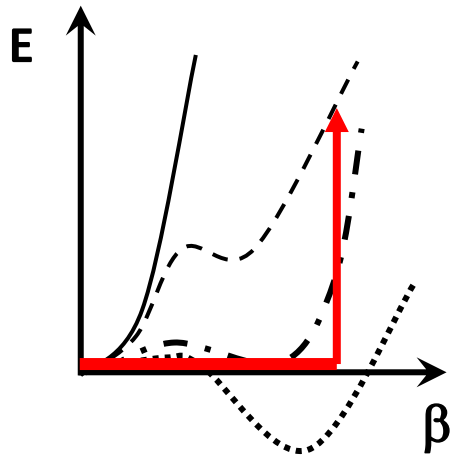


M. Klintefjord et al. Phys. Rev. C 93, 054303 (2016)

# Phase diagram of nuclear shapes

Quantum phase transitions in equilibrium shapes of nuclei

control parameters:  $N, Z$



approximation: infinite square-well potential

- analytically solvable
- certain characteristics of 1. order phase transition
- X(5) critical point symmetry

square well that is also independent of  $\gamma$

- also analytically solvable
- characteristics of 2. order phase transition
- E(5) critical point symmetry

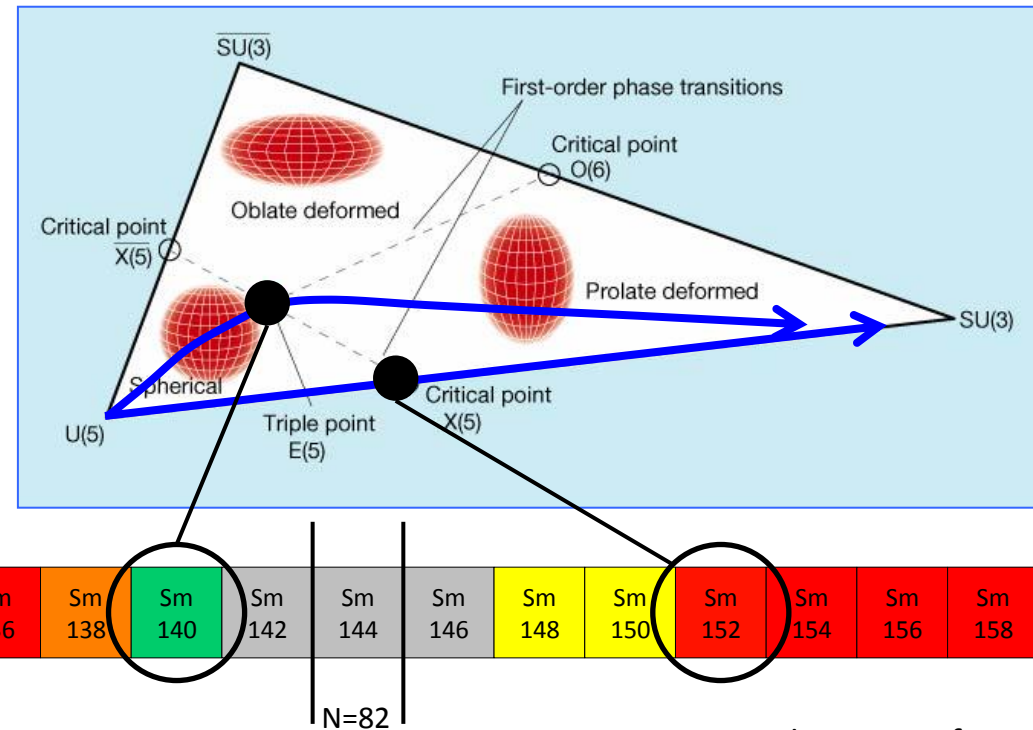
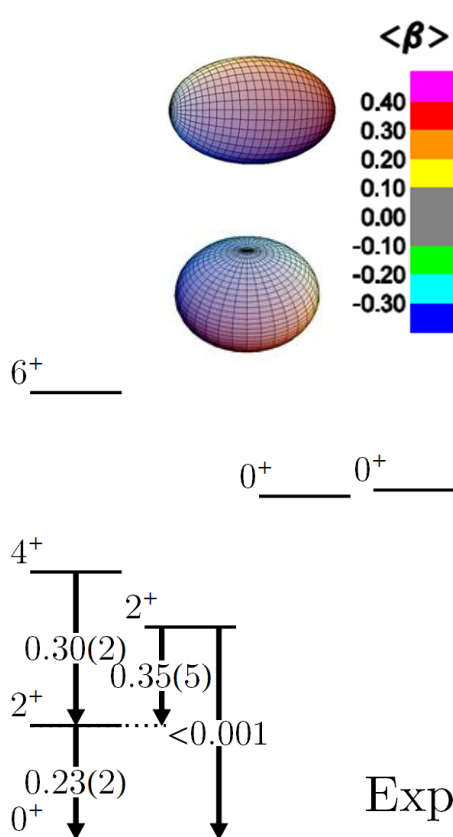
F. Iachello, Phys. Rev. Lett. 85, 3580 (2000)

F. Iachello, Phys. Rev. Lett. 87, 052502 (2001)

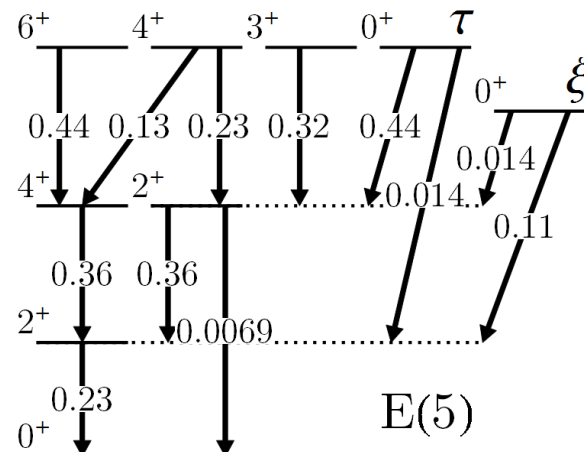
# Phase diagram of nuclear shapes

Quantum phase transitions in equilibrium shapes of nuclei

control parameters:  $N, Z$



R. F. Casten and N. V. Zamfir  
PRL 87, 052503 (2001)



new HIE-ISOLDE experiment  
August 2017

M. Klintefjord, PhD Univ. Oslo 2016

M. Klintefjord et al. Phys. Rev. C 93, 054303 (2016)